

1 **A Tropospheric Emission Spectrometer HDO/H₂O retrieval simulator for climate models**

2 **Robert D. Field^{1,2}, Camille Risi^{3,4}, Gavin A. Schmidt¹, John Worden⁵, Apostolos Voulgarakis^{1,6,7},**
3 **Allegra N. LeGrande^{1,6}, Adam H. Sobel^{2,8,9}, Richard J. Healy⁶**

4 1. NASA Goddard Institute for Space Studies, New York, NY, USA

5 2. Dept. of Applied Physics and Applied Mathematics, Columbia University, New York, NY, USA

6 3. LMD/IPSL, CNRS, Paris, France

7 4. Cooperative Institute for Research in Environmental Science, University of Colorado Boulder,
8 Boulder, CO, USA

9 5. Jet Propulsion Laboratory/California Institute of Technology, Pasadena, CA, USA

10 6. Center for Climate Systems Research, Columbia University, New York, NY, USA

11 7. Department of Physics, Imperial College, London, UK

12 8. Dept. of Earth and Environmental Sciences, Columbia University, New York, NY, USA

13 9. Lamont-Doherty Earth Observatory, Columbia University, New York, NY, USA

14 Correspondence to: R. D. Field (rf2426@columbia.edu)

15 **Abstract**

16 Retrievals of the isotopic composition of water vapor from the Aura Tropospheric Emission Spectrometer
17 (TES) have unique value in constraining moist processes in climate models. Accurate comparison
18 between simulated and retrieved values requires that model profiles that would be poorly retrieved are
19 excluded, and that an instrument operator be applied to the remaining profiles. Typically, this is done by
20 sampling model output at satellite measurement points and using the quality flags and averaging kernels
21 from individual retrievals at specific places and times. This approach is not reliable when the modeled
22 meteorological conditions influencing retrieval sensitivity are different from those observed by the
23 instrument at short time scales, which will be the case for free-running climate simulations. In this study,

1 we describe an alternative, ‘categorical’ approach to applying the instrument operator, implemented
2 within the NASA GISS ModelE general circulation model. Retrieval quality and averaging kernel
3 structure are predicted empirically from model conditions, rather than obtained from collocated satellite
4 observations. This approach can be used for arbitrary model configurations, and requires no agreement
5 between satellite-retrieved and modeled meteorology at short time scales. To test this approach, nudged
6 simulations were conducted using both the retrieval-based and categorical operators. Cloud cover, surface
7 temperature and free-tropospheric moisture content were the most important predictors of retrieval quality
8 and averaging kernel structure. There was good agreement between the δD fields after applying the
9 retrieval-based and more detailed categorical operators, with increases of up to 30 ‰ over the ocean and
10 decreases of up to 40 ‰ over land relative to the raw model fields. The categorical operator performed
11 better over the ocean than over land, and requires further refinement for use outside of the tropics. After
12 applying the TES operator, ModelE had δD biases of -8 ‰ over ocean and -34 ‰ over land compared to
13 TES δD , which were less than the biases using raw modeled δD fields.

14 **1. Introduction**

15 In order to usefully compare model predictions against satellite measurements, various features of the
16 retrieval must be taken into account. For retrievals of trace-gas profiles based on optimal estimation, these
17 are: the effects of the satellite’s orbital path, varying retrieval sensitivity under different atmospheric
18 conditions, limited vertical resolution, and contributions from a-prior constraint profiles. This involves
19 excluding profiles that would be poorly retrieved, and, for the profiles remaining, applying an instrument
20 operator to the raw model profiles. This transforms the raw model fields of interest into what would be
21 seen by the instrument. By comparing the modified profiles against the satellite retrievals, genuine model
22 errors can be more readily identified.

23 The vertical sensitivity of each retrieval to the true vertical profile is represented by an averaging kernel,
24 which depends on factors such as cloud cover and surface temperature. In applying the instrument

1 operator to the model field, the choice of quality filtering, prior and averaging kernels should be as
2 specific as possible to the model conditions at each time and location. Under the presence of thick clouds,
3 for instance, infrared retrievals are typically of poor quality and excluded from any analysis of the
4 satellite data; the same filter needs to be applied to the model data in these conditions. This is also true for
5 averaging kernel structure. For a high quality retrieval over low clouds, the peak retrieval sensitivity will
6 be at a greater height than for clear sky conditions, all other factors being equal.

7 Suitable quality filtering and averaging kernel selection is commonly assumed to be achieved by sampling
8 the model fields along the orbital path of the satellite and using information from individual retrievals.
9 The assumption underlying this approach is that the modeled meteorological conditions influencing
10 retrieval sensitivity and averaging kernel structure are in good agreement with those viewed by the
11 instrument. However, persistent differences between the observed and modeled clouds, for example,
12 would lead to unsuitable quality filtering, averaging kernel selection, and possibly inaccurate diagnostics.
13 When the quality filtering and averaging kernels selection are poor, differences between the satellite and
14 the model for the quantity of interest cannot be attributed solely to model error, which is the goal, but also
15 to this poor selection, defeating the purpose of applying the instrument operator. Selection error will
16 increase with fewer constraints on the modeled meteorology. It is presumably smaller for chemical
17 transport models (CTMs) with fully-prescribed, assimilated meteorology, and increases for coupled
18 chemistry-climate models with nudged meteorological components such as horizontal winds. For free-
19 running simulations, there is no expectation that the modeled and instrument-measured meteorological
20 fields agree at short time scales. To the best of our knowledge, however, the effect of errors in the
21 meteorology (e.g. clouds) on retrieval quality filtering and averaging kernel selection has not been
22 assessed in any of these cases.

23 Our interest is in retrievals of the deuterium composition of water vapor (HDO) from the Tropospheric
24 Emission Spectrometer (TES). These data have unique potential value in understanding moist processes
25 in the atmosphere (Sherwood et al., 2010), and for our purposes, in constraining cloud physics

1 parameterizations. For this purpose, perturbed physics tests of convective parameters with nudged winds
2 can provide a useful evaluation of the subgrid physics with realistic boundary conditions, while free-
3 running simulations are important when parameterization changes can feedback strongly onto the large-
4 scale circulation. But in the latter case, because we have no expectation of time-evolving agreement
5 between the free-running model and observed weather, the standard approach to retrieval quality filtering
6 and averaging kernel selection cannot be used reliably. This is particularly important in the case of
7 deuterium because cloud processes will strongly influence the isotopic composition of vapor, and also its
8 measurability.

9 In this study, we examine the assumptions underlying the standard, retrieval-based approach to applying
10 the TES HDO operator and describe an alternative ‘categorical’ approach for use specifically with free-
11 running climate model simulations. The categorical approach relies as little as possible on short time-
12 scale agreement between the model and instrument of quantities that influence retrieval quality and
13 averaging kernel structure. It instead uses their dependence on atmospheric conditions, similar to those
14 identified by Lee et al. (2011), in trying to predict the retrieval quality and averaging kernel structure for a
15 given set of model conditions. Our approach was also motivated by the progress made in cloud simulators
16 (e.g. Bodas-Salcedo et al., 2011) in that we apply the TES operator as an instrument simulator within the
17 NASA GISS ModelE general circulation model (GCM). Our focus is on the tropics, in order to evaluate
18 the performance of the TES operators under a limited set of conditions, and where our future process-
19 based studies will be initially conducted.

20 The paper is structured as follows. Section 2 describes the TES HDO retrievals and the factors which
21 influence retrieval quality and averaging kernel structure. The GISS ModelE is described in Section 3.
22 The standard, retrieval-based TES operator and its suitability are described in section 4. The new,
23 categorical TES operator and its suitability are described in section 5. In section 6, the effects of applying
24 the two types of TES operators on the modeled δD fields are examined, several sensitivity tests are

1 described, and the retrieved and modeled δD fields are briefly compared. A brief discussion follows in
2 section 7. Future studies will examine the reasons for model-satellite δD discrepancies in detail.

3 **2. TES HDO/H₂O retrievals**

4 **2.1 TES HDO retrieval and instrument operator**

5 The TES instrument onboard the Aura satellite is an infrared Fourier transform spectrometer measuring in
6 the 650 cm⁻¹ to 3050 cm⁻¹ spectral range, following a sun-synchronous orbit with a repeat cycle of 16 days
7 (Beer et al., 2001). We use version 4 level 2 H₂O and HDO nadir retrievals which have a horizontal
8 footprint of 5.3 km by 8.5 km. H₂O and HDO concentrationamounts are jointly retrieved using optimal
9 estimation, using spectral windows in the region between 1100 cm⁻¹ and 1350 cm⁻¹ (Worden et al., 2006).

10 The retrieved profiles represent an adjustment from the prior H₂O and HDO constraint profiles. The
11 adjustment is estimated iteratively to minimize the difference between the measured spectra and that
12 predicted by a forward radiative transfer model using the estimated profiles as input (Clough et al., 2006).
13 Retrieved profiles are provided on 67 pressure levels.

14 For HDO, a single, constant HDO/H₂O profile from the global mean of the NCAR CAM model is used
15 for the prior constraint. For H₂O, the prior varies by retrieval, and is obtained from collocated grid points
16 from the GEOS-5 global transport model~~ed~~ operated by the NASA Global Modeling and Assimilation
17 Office (GMAO) (Rienecker et al., 2007). A single, fixed H₂O constraint would yield poor-quality
18 retrievals because H₂O concentrationamount can vary so widely in the troposphere. The retrieval is based
19 on the logarithm of H₂O and HDO profiles because of their potentially large variation in the vertical, and
20 to ensure positive retrieved concentrationamounts. The estimated error of the retrieved HDO is 10% in the
21 tropics (Worden et al., 2007**b**). All analysis is for daytime retrievals only, for compatibility with the
22 simulated ISCCP cloud properties (described in Sect. 3).

1 The TES HDO instrument operator applied to model profiles can be described as follows. Using the
 2 notation of Worden et al. (2011), the model HDO/H₂O ratio \hat{x}_R suitable for comparison with satellite
 3 measurements is expressed as

$$\hat{x}_R = x_a^R + (A_{DD} - A_{HD})(x_D - x_a^D) - (A_{HH} - A_{DH})(x_H - x_a^H). \quad (1)$$

4 In Eq. (1), the subscripts and superscripts indicate the following: R relates to the isotopic ratio HDO/H₂O,
 5 a relates to a ~~prior constraint~~ *a priori constraint*, D relates to HDO and H relates to H₂O. In Eq. (1), x_a^R
 6 is the prior isotopic ratio HDO/ H₂O before standardization with respect to Vienna Standard Mean Ocean
 7 Water (VSMOW), x_a^D is the prior HDO ~~concentration amount~~ and x_a^H is the prior H₂O
 8 ~~concentration amount~~. x_D and x_H are the raw, modeled HDO and H₂O ~~concentration amounts~~,
 9 respectively. All x terms are the logarithm of the isotopic ratio or species ~~concentration amount~~, i.e., $x =$
 10 $\ln(q)$, where q is the species ~~concentration amount~~ in units of volume mixing ratio (vmr). The x terms are
 11 column vectors of size 67x1, with modeled ~~concentration amounts~~ interpolated linearly from the 40 model
 12 levels. A_{DD} is the HDO averaging kernel, A_{HH} is the H₂O averaging kernel, and A_{HD} and A_{DH} are the
 13 cross-kernels between them. The cross kernels represent the sensitivity of one retrieved species to the
 14 actual profile of the other. All averaging kernels are square but asymmetric matrices with size 67x67.
 15 Following Risi et al. (2012), the full 67 TES pressure levels were truncated to the vertical range relevant
 16 to HDO analysis. The \hat{x}_R and x_a^R vectors were truncated to the 10 TES pressure levels spanning the 909
 17 hPa to 383 hPa range, where the HDO retrievals are somewhat sensitive. The x_a^D , x_a^H , x_D and x_H
 18 vectors were truncated to the 26 TES levels spanning the 1000 to 100 hPa range, HDO and H₂O
 19 composition over which can influence the retrievals over 907 hPa to 383 hPa. Accordingly, each of the
 20 averaging kernel matrices is truncated to size 10x26. This truncation reduces computation time and
 21 storage requirements for the TES data considerably, with little effect on the results (Risi et al., 2012).
 22 Most analysis presented in this study is further restricted to the 825 hPa to 510 hPa range where the HDO
 23 retrieval is most sensitive, following Yoshimura et al. (2011), ~~and which spans the ~600 hPa level~~

1 | [examined by Berkelhammer et al. \(2012\) and Risi et al. \(2012\)](#). TES measurements were mapped to the 2°
2 | x 2.5° ModelE grid.

3 | The overall sensitivity of the retrieval is measured by the trace of the HDO averaging kernel A_{DD} . HDO
4 | retrieval sensitivity is influenced by cloud thickness and height, surface temperature and moisture content
5 | (Worden et al., 2011). Only retrievals classified as high quality [are included, which was defined as having](#)
6 | ~~and with~~ sensitivity greater than 0.5 ~~are included~~ (Lee et al., 2011; Berkelhammer et al., 2012; Risi et al.,
7 | 2012) [and the overall HDO retrieval quality flag set to 1](#). The minimum sensitivity requirement ensures
8 | that the retrieval is sufficiently sensitive over some vertical range to the measured spectra, and not
9 | dominated by contributions from the prior constraint. Fig. 1 shows an example TES nadir orbital path
10 | during daytime over the tropics for one day. Of 133 measurements, only the 85 high-quality retrievals are
11 | shown. Example averaging kernels for one high quality retrieval over the Indian Ocean are shown in Fig.
12 | 2. After the quality filtering, we adopt the pressure level of peak sensitivity for a given level of retrieved
13 | HDO, defined as p_D , as the key characteristic of the operator. In Fig. 2a, p_D for both the 619 hPa (purple)
14 | and 681 hPa (light blue) is approximately 700 hPa. The mean p_D between 825 hPa and 510 hPa will be the
15 | primary metric used for distinguishing averaging kernel shapes.

16 | Fig. 3 shows the spatial variation of retrieval quality and p_D across the tropics during 2006-2009. There
17 | were 202 713 daytime retrievals, 69% of which were high quality over the ocean and 57 % over land, but
18 | with considerable spatial variation (Fig. 3a). Over the oceans, there ~~is lower were fewer high-quality~~
19 | ~~retrieval quality~~s over the ITCZ and SPCZ bands, eastern Indian Ocean, the Maritime Continent, and the
20 | West Pacific Warm Pool due to the frequent presence of precipitating clouds. There is also lower retrieval
21 | quality off of the west coasts of South America and Africa possibly due to low moisture content and
22 | lower sea-surface temperatures. Over land, the lowest quality is over the Sahara, presumably due to low
23 | moisture content. Given that the retrieval quality can decrease under either very wet or very dry
24 | conditions, there is no apparently simple rule which would separate low and high quality retrievals.

1 Over 825 hPa to 510 hPa, there is also considerable variation in p_D for high quality retrievals (Fig. 3b).
2 Over the oceans, p_D is lower (at a higher altitude) in moist regions where there is abundant mid
3 tropospheric moisture, but also in the dry regions off of the coasts of South America and Africa
4 presumably due to low-level marine stratocumulus, as described by Lee et al. (2011). p_D is higher over
5 the dry subtropical anticyclones due to a moist boundary layer and dry free troposphere.

6 **2.2 Observed controls on TES HDO retrieval quality and p_D**

7 The first task in developing the new approach is to understand controls on retrieval quality and p_D in the
8 TES measurements. Possible controls were identified using the pattern correlations between Fig. 3a and
9 Fig. 3b and different underlying meteorological quantities. The following variables were considered from
10 mean fields calculated from 2006-2009: cloud optical depth (τ), cloud fraction (CF), defined as the
11 percentage of retrievals in a grid cell with cloud optical depths greater than 0.3, cloud top pressure (CTP),
12 surface temperature (T_S), and moisture content. Moisture content was expressed as total precipitable water
13 (PW_T) and further separated into precipitable water in the boundary layer (PW_B) (within 150 hPa of the
14 surface) and precipitable water in the free atmosphere (PW_F) (above 150 hPa from the surface). All
15 moisture quantities were computed from the prior H₂O profiles, which are sampled from GMAO
16 reanalysis. The analysis of controls on p_D is for high quality retrievals only, for both the averaging kernels
17 and underlying meteorological quantities. Correlation and regression quantities were computed using
18 ordinary least-squares regression, which does not take into account errors in the control variables.

19 Table 1 lists the pattern correlations. Over the ocean, retrieval quality was most strongly associated with
20 CF , with a correlation of -0.70, indicating that, as would be expected, retrieval quality decreases with
21 increasing cloud cover. Compared to CF , τ was a weak predictor of retrieval quality, likely because of its
22 highly non-normal distribution. Over land, retrieval quality was most strongly associated with T_S , with a
23 correlation of -0.72 and to a slightly lesser degree, with PW_B , (which itself has a correlation of -0.59 with
24 T_S). Over the ocean, p_D is most strongly associated with PW_F . As PW_F decreases, p_D moves toward the
25 boundary layer where moisture content is generally abundant, and will therefore exert a stronger influence

1 on the retrieved HDO at higher altitudes. PW_B itself had a low correlation with p_D because it varies
2 substantially less than PW_F over the ocean. Over land, p_D was most strongly associated with T_S , but with
3 a lower correlation of -0.51 compared to over ocean, and equally high correlation with PW_F .

4 The linear fits between retrieval quality and p_D for the primary control variables are shown in Fig. 4. It
5 can also be seen that the observed control on retrieval quality over land is due to a set of high-
6 temperature, low quality points, which were associated with extremely hot and dry conditions over the
7 Sahara (Fig. 3a). The unexplained variation in these relationships is due to the influence of the more
8 weakly correlated variables and other unknown factors. We considered adopting multivariate regression
9 models to capture this variability, but found that the collinearity between meteorological quantities led to
10 unstable regression estimates, and that remedial measures such as principal component regression
11 precluded straightforward interpretation.

12 Comparisons such as those in Fig. 4 will serve as the primary means of evaluating the suitability of
13 different TES operators. It is these relationships that we seek to evaluate for different TES HDO operators
14 in the model, namely that:

- 15 | - Retrieval quality should decrease where there is increasing CF over ocean, and increasing T_S over
16 | land.
- 17 | - p_D should move closer to the boundary layer as PW_F decreases over the ocean, and move closer to
18 | the free troposphere as T_S decreases over land.
- 19 | - The scatter in the linear fits is similar to that observed in the TES measurements. That is, the
20 | dispersion of the residuals around the fitted regression lines should be similar to those in Fig. 4.

21 3. NASA GISS ModelE

22 | We use the atmosphere-only version of the NASA GISS ModelE general circulation model at $2^\circ \times 2.5^\circ$
23 | horizontal resolution and 40 vertical levels. The core model is an updated version of that described in

1 Schmidt et al. (2006), with a recent summary of the cloud physics provided by Kim et al. (2011). The
2 simulation period was 2006-2009, covering the continuous period of TES retrievals, with an additional
3 year for spin-up. A spin up time of five years did not affect the results. Internationally-varying monthly
4 sea-surface temperatures and sea-ice cover are prescribed (Rayner et al., 2003). The horizontal winds in
5 the model were nudged toward NCEP-NCAR Reanalysis (Kalnay et al., 1996) at each model time-step.
6 All other dynamical quantities are calculated prognostically. Our eventual interest is evaluation of free-
7 running simulations against the TES observations, but nudging allowed for consistent comparison
8 between the retrieval-based and categorical TES operators for a configuration typical of how the retrieval-
9 based operator has been commonly applied in the past.

10 ModeLE is equipped with stable water isotope tracers (Schmidt et al., 2005), advected using the quadratic
11 upstream scheme of Prather (1986), which yields an effective transport resolution approximately twice
12 that of the horizontal model resolution. Isotopic fractionation between H₂O and the rare isotopologues
13 H₂¹⁸O and HDO is parameterized for all moist processes, from evaporation and evapotranspiration over
14 the ocean and land surfaces, to condensation and deposition, and post-condensation exchange between
15 rainfall and vapor. The stable water isotope tracer parameterization is much simpler than the underlying
16 cloud parameterization, and is more tightly constrained by laboratory measurements. This is what makes
17 the TES HDO retrievals potentially valuable, as isotopic measurements can be used in evaluating the
18 underlying cloud physics with a fair amount of confidence that the isotopic physics are correct. Or, put
19 another way, errors in the modeled isotopic fields are likely to be dominated by errors in the cloud
20 physics rather than errors in the isotopic physics.

21 ModeLE also includes an internal simulator for the International Satellite Cloud Climatology Project
22 (ISCCP) that produces cloud diagnostics for comparison with the ISCCP datasets (Klein and Jakob,
23 1999). For our purposes, the key feature of the ISCCP simulator is the random, subgrid joint distribution
24 of τ and *CTP*, conditioned upon the grid-scale vertical distributions of humidity, convective cloud cover
25 and large-scale cloud cover.

1 **4. Retrieval-based TES HDO operator**

2 **4.1 Review of retrieval-based operators in previous studies**

3 | In applying the TES operator in Eq. (1) to model profiles \mathbf{x}_D and \mathbf{x}_H , choices must be made whether to
4 | include the profile, in choosing the prior profile \mathbf{x}_a^H , and the averaging kernels \mathbf{A}_{DD} , \mathbf{A}_{HH} , \mathbf{A}_{HD} and \mathbf{A}_{DH} ,
5 | all of which are different for each retrieval. These choices should reflect the conditions at each model
6 | point. Using the standard, retrieval-based approach, the model fields are sampled along the orbital path,
7 | but excluding model points collocated with poor-quality retrievals. For the remaining model points, the
8 | averaging kernels and priors from individual measurements are used in applying Eq. (1). The underlying
9 | assumption of this approach is that the modeled and retrieved factors influencing retrieval quality and
10 | averaging kernel structure are in agreement.

11 | This approach is based on the earlier, pre-Aura launch description of Jones et al. (2003) of the potential
12 | accuracy of the TES CO retrievals. Variants of the technique have been used in validating TES retrievals
13 | against collocated measurements of CO from aircraft (Luo et al., 2007a), O₃ from aircraft (Richards et al.,
14 | 2008) and sondes (Worden et al., 2007a), and H₂O measurements from sondes (Shepherd et al., 2008). It
15 | has also been used for comparisons between TES CO retrievals and those from the Atmospheric
16 | Chemistry Experiment (ACE) (Rinsland et al., 2008) and Measurements of Pollution in the Troposphere
17 | (MOPITT) (Luo et al., 2007b).

18 | The approach has subsequently been applied in CTM studies focusing on TES O₃ data assimilation
19 | (Parrington et al., 2008), the sources, sinks and transport of pollution in the troposphere (Nassar et al.,
20 | 2009; Choi et al., 2010; Liu et al., 2009), and inverse modeling of CO (Jones et al., 2009) and CO₂
21 | (Nassar et al., 2011). These studies all involved CTMs with fully prescribed meteorological fields. In
22 | studies using the GEOS-Chem CTM, meteorology is prescribed from GMAO reanalysis. Through its
23 | assimilation of radiosonde profiles of temperature, humidity and winds, and independent satellite
24 | estimates of atmospheric moisture and winds, the GMAO reanalysis provides reasonable estimates of the

1 factors which are known to influence averaging kernel structure and retrieval sensitivity (e.g. Norris and
2 Da Silva, 2007).

3 Voulgarakis et al. (2011) applied the TES operator using the retrieval-based approach in their analysis of
4 O₃-CO correlations for two coupled chemistry-climate models with prescribed SSTs and horizontal winds
5 nudged toward reanalyses. All other meteorological fields were calculated prognostically, unlike the CTM
6 studies described above. Aghedo et al. (2011) considered three chemistry-climate models with prescribed
7 SSTs and nudged toward reanalysis, and using collocation-based averaging kernel selection and quality
8 filtering. A fourth free-running (non-nudged) simulation was also considered. Their focus was on
9 estimating the error associated with using monthly mean maps of spatially-varying averaging kernels
10 rather than individual retrievals. A small error would allow the TES operator to be applied to monthly
11 mean model output, simplifying multi-model comparisons against satellite measurements. We note that
12 by embedding the TES operator within the model, we have avoided this issue altogether.

13 Risi et al. (2012) used the monthly-mean approach in comparing TES HDO fields to those from nudged
14 simulations with the LMDz isotopically-equipped GCM for several different ~~model~~
15 ~~configurations~~ parameter values within the cloud scheme. Yoshimura et al. (2011) used the standard
16 approach using individual retrieval-based sampling in their comparison of the TES and IsoGSM HDO
17 fields with varying isotopic physics, noting that this approach necessitates model nudging. Both studies
18 stressed the importance of applying the TES operator to model outputs for quantitative comparisons with
19 the data. Lee et al. (2009) and Field et al. (2010) compared TES HDO to free-running simulations with
20 different convective and isotopic configurations, but without applying a TES operator, making their
21 interpretation necessarily qualitative.

22 **4.2 Retrieval-based controls on TES HDO retrieval quality and p_D**

23 | The standard, retrieval-based TES operator was implemented within ModelE for ~~the~~-H₂O and HDO. TES
24 | retrievals are ingested into the model's TES simulator along Aura's orbital path (as in Figure 1) at each

1 half-hour model time step, during daytime and over the tropics only. The retrieval quality filtering and
2 averaging kernel selection is done regardless of the agreement in meteorology between the model and
3 TES. In cases where a model cell contains more than one high quality TES measurement, the averaging
4 kernels and H₂O priors for all are applied to the model profile and the mean of the resulting profiles is
5 taken.

6 We evaluated the suitability of this approach by comparing the relationships in Table 1 for the TES
7 observations to those from the retrieval-based operator. If the modeled meteorology agreed exactly with
8 that retrieved by the instrument, then the relationships between retrieval quality and p_D would be the same
9 as in Table 1 when the control variables from TES are replaced with those from the model. The degree to
10 which this is not the case quantifies the difference in meteorology observed by TES and simulated by the
11 model in the context of their influence on retrieval quality and p_D .

12 Fig. 5 shows the same observed TES retrieval quality and p_D as Fig. 4, but as a function of modeled CF
13 and PW_F over the ocean and T_S over land. Over the ocean, there is too weak a decrease in observed
14 retrieval quality with increasing model CF , indicated by the slope of -0.18 and weaker correlation of -
15 0.26 (Fig. 5a). This reflects, despite nudging, the low correlation of 0.35 between the TES and ModelE
16 CF . The regions where TES is excluding more retrievals do not always correspond to where the thick
17 clouds are in the model, for example. There is less disagreement in control on retrieval quality over land
18 (Fig. 5c), because of the higher correlation of 0.74 between modeled and retrieved T_S . Compared to
19 retrieval quality, the observed controls on p_D over the ocean are better captured by the retrieval-based
20 operator (Fig. 5b). This is also due to the strong correlation between the TES and ModelE ocean PW_F
21 fields (0.86), which leads to a similar relationship with p_D . Over land, the relationship between modeled
22 T_S and p_D is in fair agreement with, but slightly weaker than for the observed T_S .

1 **5. Categorical TES HDO operator**

2 **5.1 Description of categorical operator**

3 The observed TES retrieval quality and, to a lesser extent p_D , are not entirely consistent with the
4 underlying model conditions, despite nudging. This problem will be worse for free-running simulations.
5 We have therefore developed a technique to apply the TES operator in a way that presumes no agreement
6 between the observed and modeled meteorology at short time-scales, but such that the retrieval quality
7 and averaging kernel selection are suited to the modeled conditions at that point. This approach is referred
8 to as the ‘categorical operator’ and was implemented alongside the retrieval-based operator in ModelE.

9 For different categories defined according to the variables in Table 1, we computed the mean retrieval
10 quality, mean averaging kernels, and mean H₂O prior from the TES retrievals (described in detail in the
11 next section). The mean retrieval quality is the proportion of HDO retrievals in a category that were
12 classified as high quality. The mean of the averaging kernels is the matrix resulting from taking the
13 element-by-element means of all averaging kernels (for high quality retrievals only) falling into a given
14 category. Applying the categorical TES operator in the model then consists of two steps:

- 15 1. At each time step and grid point, the values of the categorical variables in the model are used to
16 look up the associated categorical TES retrieval quality. The model profile is included with a
17 probability equal to the categorical retrieval quality. ~~That is, if~~ a particular set of model
18 conditions ~~were was~~ associated with 30% high quality retrievals, for example, then there is a 30%
19 chance that that model profile would be included.
- 20 2. For the profiles passing the retrieval quality filter, the categorical variable values in the model are
21 used to look up the associated prior H₂O profile and averaging kernels, which are used in
22 applying Eq. (1).

23 Thus, rather than use information from individual retrievals, we use conditions in the model to
24 empirically predict the retrieval quality and averaging kernel structure for a sampled model point.

1 5.2 TES categorizations

2 Thirteen categorizations of increasing complexity were considered, which ranged from having one
3 category across all retrievals to 1620 categories when the retrievals were separated according to discrete
4 ranges of all control variables. Table 2 shows the values used for each variable in different
5 categorizations. *CF* is not retrieved for individual measurements, but is included implicitly for the
6 categories involving clouds by including a clear sky category with τ less than 0.3. An important element
7 of the categorical operator is our use of the ISCCP simulator in ModelE. Rather than use grid-mean
8 values of τ and *CTP*, we randomly select an ISCCP subgrid column with equal probability and use its τ
9 and *CTP*. The subgrid τ will not be normally distributed; a single, large τ can skew an otherwise clear-
10 sky grid box toward an unrepresentatively high τ in the grid-scale mean. Using the individual ISCCP
11 subgrid columns guards against an inevitable bias toward high τ values with low retrieval sensitivity that
12 would result if the grid-scale mean were used. Inclusion of low sensitivity retrievals would result in
13 comparison of retrieved and, after applying the TES operator, model profiles that have both relaxed
14 toward the prior, creating artificially high agreement between the satellite and model (Nassar et al., 2008).

15 | Categorizations are named according to the variables they include. We tried to strike a balance between
16 | capturing distinctions in retrieval quality and averaging kernel structure and using as few categories as
17 | possible. The cloud-only C categorization extends the decomposition of Lee et al. (2011) to the coarse,
18 | qualitative ISCCP categories. The C_fine categorization corresponds to the full ISCCP categories. The
19 | PW and PW_fine categorizations use precipitable water only, and contribute 9 and 49 categories
20 | respectively when precipitable water is separated into boundary layer and free-atmosphere components.
21 | The LO τ TPW_F categorization with 180 categories included only the variables identified in Table 1 as the
22 | most important (land/ocean separation, τ , T_s and PW_F). This was a possible optimal categorization that
23 | captures variation in retrieval quality and p_D using far fewer categories than the full LOCTPW
24 | categorization which includes all variables.

1 To show how retrieval quality and averaging kernel structure varies, we look first at the C categorization
2 based on τ and CTP . Retrievals with τ less than 0.3 account for 64% of observations, with the rest
3 consisting mostly of mid- and high-level clouds (Table 3). Retrieval quality is generally high for τ less
4 than 1.3, and for low-level clouds with τ between 1.3 and 3.6 (Table 4), but otherwise poor. The
5 relatively poor quality of 68.2% for the low τ and high CTP category suggests an additional factor
6 influencing retrieval quality, such as T_S over land.

7 To illustrate the associated changes in averaging kernel structure, Fig. 6 shows the averaging kernel rows
8 at 619 hPa for CTP less than 440 hPa and three different ranges of τ . Averaging kernels rows for τ less
9 than 0.3 (Fig. 6a) have a higher p_D than for τ between 0.3 and 1.3 (Fig. 6b), but neither peak is
10 particularly sharp. Neither is significantly different from the grand mean because these categories
11 constitute such a large proportion of all retrievals. Sensitivity for thicker clouds is generally low (Fig. 6c),
12 even with only high quality retrievals included, and the averaging kernel has a much flatter peak. The
13 average retrieval quality for this category is 11%. Model points corresponding to these conditions would
14 in general be excluded from the analysis.

15 The CPW categorization extends the C categorization by further separating the retrievals according to
16 PW_B and PW_F , which may vary independently of cloud cover. Fig. 7 shows the averaging kernels
17 underlying the mean in Fig. 6a, but for a moist boundary layer (PW_B greater than 20mm) and for three
18 categories of PW_F . The main distinction is that p_D increases from 600 hPa in Fig. 7a to 800 hPa in Fig. 7c
19 as PW_F decreases. The error bars are also narrower than in Fig. 6a, and particularly for the low PW_F case,
20 the peaks are sharper than in separating based on τ only in Fig. 6a and Fig. 6b. Although the focus of the
21 averaging kernel separation is the A_{DD} row at 619 hPa, the corresponding changes in the H₂O prior x_a^H
22 (not shown) were as expected, with the x_a^H decreasing strongly above the boundary layer for PW_F less
23 than 10mm.

1 Before applying the TES operator, we can gauge how more complicated categorizations might yield a
2 better mapping from model conditions to retrieval quality and the most suitable averaging kernels. Of
3 interest is the degree to which different categorizations separate high from poor quality retrievals, and for
4 the high quality retrievals, the degree to which p_D is separated. This is analogous to the correlations in
5 Table 1, but for a set of discretized predictor variables.

6 For each categorization, the separation between high and poor quality retrievals was measured by the
7 mean difference between each category's quality and the overall mean quality. In computing the mean
8 difference, each categorical quality is weighted by the number of observations, so that low-quality
9 categories with few observations are not over-represented. For the C categorization, this value is 18.4%,
10 the mean of the absolute differences between the entries in Table 4 and the overall mean of 68%, with the
11 mean absolute difference in each category weighted by the frequency of occurrence entries in Table 3.

12 Fig. 8 shows this value for each of the ~~thirteen~~twelve categorizations. Most of the separation in retrieval
13 quality can be obtained using only the simple 'C' categorization, with smaller contributions from other
14 variables. This is consistent with the strong pattern correlation between retrieval quality and cloud
15 fraction in Table 1. The strongest additional gains are made by including T_S in the categorization (CT),
16 consistent with its association with retrieval quality over land. Despite the importance of cloud properties
17 in separating good retrievals from bad, little was gained by using the 'C_fine' categorization, which is
18 likely due to the larger error in the cloud properties (Eldering et al., 2008) compared to other categorical
19 variables.

20 Averaging kernel separation was measured by the total root-mean square error (RMSE) of p_D at 619 hPa
21 across all categories in a categorization. Only high quality retrievals were considered in calculating the p_D
22 RMSE for consistency with any analysis of the retrieved HDO fields. The p_D RMSE can be thought of as
23 the total, within-category standard deviation of p_D across all categories, weighted by frequency of
24 occurrence. We are interested in the degree to which the total within-category variance p_D decreases for
25 increasingly complicated categorizations, or how the error bar widths tend to decrease across all

1 categories within a categorization. A decrease in the p_D RMSE would result in a better mapping between
2 model conditions and averaging kernel shape.

3 Fig. 9 shows the total p_D RMSE for the thirteen different categorizations. Precipitable water plays a more
4 important role in separating p_D than in separating retrieval quality. The PW categorization, for example,
5 contributes to greater p_D separation than the C categorization, despite having fewer categories. There is a
6 further decrease for the CPW categorization, and also for the CTPW categorization. The ‘LO τ TPW_F’
7 categorization appears to strike a balance between minimizing the RMSE and using relatively few
8 categories, with further, slight decreases for the CTPW and full LOCTPW categorizations.

9 From Fig. 8 and Fig. 9, all of clouds, precipitable water and surface temperature are important, which we
10 would expect from Table 1. The cloud categories are important on their own in separating high from poor
11 quality TES retrievals, and precipitable water provides most separation of p_D . There are diminishing
12 returns, however, as the size of the categorization increases. It is not immediately clear whether more
13 complicated categorizations yield relationships closer to those in Table 1 or different δD fields after
14 applying the TES operator.

15 **5.3 Categorical controls on TES HDO retrieval quality and p_D**

16 | The categorical operator was tested in ModelE with ~~five-four~~ representative categorizations: C, PW,
17 | ~~CPW~~, LO τ TPW_F and LOCTPW. In each case, the underlying model configuration was the same as in the
18 | case of applying the retrieval-based TES operator, but the quality filtering and averaging kernel and H₂O
19 | prior selection from individual TES measurements were replaced with categorical selection.

20 | Fig. 10 shows the approximated retrieval quality for the ~~five-four~~ categorizations. For the C categorization
21 | (Fig. 10a), the approximated retrieval quality bears some resemblance to the observed retrieval quality
22 | (Fig. 3a), but is 10% lower over the ocean and without the sharp decrease in retrieval quality over the
23 | southern Sahara. Over the Pacific and Atlantic sectors, the regions of high retrieval quality are ~~to the~~ east
24 | of those in the observations. The PW categorization (Fig. 10b) results in a mean ocean retrieval quality of

1 | 68.9%, nearly identical to the TES observations, but lacks the distinction between wet and dry regions ~~is~~
2 | seen in the observations and for the C categorization. The approximated retrieval quality of the ~~CPW~~,
3 | $LO\tau TPW_F$ and LOCTPW categorizations (Fig. 10c-e, d) are all similar over the ocean, with the
4 | LOCTPW categorization having a sharper decrease over the southern Sahara.

5 | While instructive to see the sensitivity of the retrieval quality to the different categorizations, their
6 | performance should, strictly speaking, be evaluated according to how well they approximate the observed
7 | relationships in Fig. 4, rather than by their agreement with the observations in Fig. 3a. These relationships
8 | are shown for the ~~five-four~~ categorizations in Fig. 11. The C categorization (Fig. 11a) results in a slightly
9 | stronger relationship ($r = -0.78$) between the cloud fraction and the approximated retrieval quality than in
10 | the observations. This would be expected given that clouds are the only categorical variable used to select
11 | quality; in the absence of other, real, complicating factors, the approximated relationship is slightly too
12 | strong compared to the observed relationship in Fig. 4a. Furthermore, over the ocean, the lower
13 | approximated retrieval quality of 58.9% is the result of the higher modeled CF (47.8%) compared to the
14 | TES observations (35.3%).

15 | Conversely, the PW categorization results in a weaker relationship between CF and retrieval quality (Fig.
16 | 11b). In this case, cloud fraction acts as a lurking variable in the categorization. CF is somewhat
17 | correlated with PW_B (0.48) and PW_F (0.67), but not strongly enough to accurately predict retrieval quality
18 | when excluded from the categorization. This case reinforces the need to evaluate the categorical operator
19 | based on agreement in the relationships, rather than in the retrieval quality fields. Over the ocean, it is
20 | tempting to infer that the PW categorization is more accurate because of its agreement in the mean (Fig.
21 | 10b) with retrieval quality. This agreement is misleading however; by not including clouds explicitly in
22 | the categorization, the approximated retrieval quality does not decrease under the higher modeled cloud
23 | fraction, which it should. The relationships are in better agreement, neither too strong nor too weak, for
24 | the $LO\tau TPW_F$ categorization (Fig. 11c), and to some extent the ~~CPW and~~ LOCTPW categorization (Fig.
25 | 11d) s. Over land, the C and PW categorizations (Fig. 11 e, f) performed poorly in capturing the variation

1 in retrieval quality over land. When T_S is not included in the categorization, there is too little covariation
2 between T_S and either of CF , PW_F or PW_F to capture the decrease in retrieval quality with T_S . More
3 realistic approximations were obtained for the $LO\tau TPW_F$ and $LOCTPW$ categorizations (Fig. 11 g, h),
4 which include T_S , and land/ocean separation, although there is still less agreement than for over the
5 ocean. Over land, the most realistic approximations were for the $LO\tau TPW_F$ and $LOCTPW$ categorizations,
6 although there is less agreement than over the ocean.

7 The approximated p_D for the five categorizations is shown in Fig. 12. The approximated p_D for the C
8 categorization (Fig. 12a) shows little of the variation seen in the TES observations (Fig. 3b), with little
9 increase in p_D over the Pacific and Atlantic subtropical anticyclones. The PW categorization (Fig. 12b)
10 does capture this increase, but not the lower p_D over the tropical rain belts, and with a smoother structure
11 owing to the smoothness of the quality filtering. The approximated p_D for the ~~CPW~~, $LO\tau TPW_F$ and
12 $LOCTPW$ categorizations (Fig. 12 c,d) were comparably similar to the TES p_D fields -over the ocean,
13 with the latter two more similar over and land.

14 Fig. 13 shows the approximated controls on p_D . As in the observed relationships in Fig. 4b and Fig. 4d,
15 PW_F and T_S include only model points classified as having high retrieval quality. The weak slope of the C
16 categorization over the ocean (Fig. 13a) reflects the absence of variation in p_D in Fig. 12a. The slope for
17 the PW categorization (Fig. 13b) is closer to the observed slope, but with an overly strong correlation, too
18 little scatter, and with unrealistically high p_D overall. Similar to retrieval quality, the control on p_D is more
19 realistic when both clouds and precipitable water are included (Fig. 13c-e,d). The inclusion of clouds in
20 the categorization helps to separate high PW_F for clear and cloudy sky, allowing the clear sky values with
21 higher quality to be included. The full $LOCTPW$ categorization has a more realistic amount of scatter, but
22 all three of CPW, CTPW and $LOCTPW$ both that and the $LO\tau TPW_F$ categorizations -have a steeper slope
23 and higher correlation than in the observations. The retrieval-based operator in Fig. 5b, by contrast, had a
24 too-flat slope and weak correlation. Over land, the approximated T_S control on p_D was of the opposite

1 | sign for the ~~C_s~~ and ~~PW_F~~ and ~~CPW~~ categorizations (Fig. 13 e, f), and best approximated by the full
2 | LOCTPW categorization (Fig. 13h).

3 | Overall, the LO τ TPW_F and LOCTPW categorizations performed best in approximating controls on
4 | retrieval quality and p_D . Both were equally deficient in not having a strong enough decrease in retrieval
5 | quality with T_s over land, and an overly strong increase in p_D with PW_F over the ocean. These are likely
6 | the greatest source of selection error in applying the categorical TES operator to raw model δD fields.

7 | **6. TES operator effects on δD fields**

8 | **6.1 Comparison of retrieval-based and categorical TES operators**

9 | Ultimately, we are interested in the effects of applying the different TES operators to raw ModelE δD
10 | fields. Fig. 14 shows this effect for the retrieval-based TES operator over the whole analysis period.
11 | Again, the retrieval-based operator has been applied regardless of agreement between the retrieved and
12 | modeled values of CF , PW_F and T_s . The effect of sampling along the orbital path can be seen by the less
13 | smooth field of Fig. 14b compared to Fig. 14a. Application of Eq. (1) to the raw model fields after quality
14 | filtering results in an average δD increase of 8.8 ‰ over ocean and 6.4 ‰ over land (Fig. 14c), but this
15 | reflects larger regional changes. In general, the largest absolute changes occur where there is the largest
16 | difference between the raw model field and the prior δD over 825 hPa to 510 hPa, which is roughly -150
17 | ‰ when vertically weighted by specific humidity. Over northern Africa, the high model δD decreases
18 | toward the prior by up to 40 ‰, whereas over South America and the Maritime Continent the low δD
19 | increases toward the prior by up to 35 ‰.

20 | Fig. 15 shows the result of applying the different categorical TES operators. The changes in δD are
21 | similar to the retrieval-based operator in that regions of low raw ModelE δD tend to increase toward the
22 | TES prior, but there are significant regional differences for the C and PW categorizations. Using the C
23 | categorization (Fig. 15a), there is a strong decrease in δD over the anticyclones in the Pacific and

1 Atlantic, despite the raw ModelE δD not being particularly high. This is due to the effect of not including
2 PW in the categorization and consequently not capturing the variation in p_D . Using only clouds in the
3 categorization, these regions are simply classified as having low CF , and will be associated with
4 averaging kernel shapes similar to those in Fig. 6a. This averaging kernel is inappropriate, however, as it
5 does not capture the higher p_D associated with the PW_F less than 10mm (Fig. 7c) which occurs in those
6 regions. As a result, the mid-tropospheric δD composition, which is low, has an overly strong influence in
7 applying Eq. (1), resulting in an overly strong δD decrease. Using the PW categorization (Fig. 15b), this
8 problem is absent, but there is a weaker increase in δD over the western Pacific warm pool. The
9 ~~remaining~~, more complex categorizations result in similar changes to the δD field (Fig. 15c-d), not
10 varying by more than 1 ‰ in their overall mean and with only small regional differences. With a
11 sufficient CF control on retrieval quality and PW_F control on p_D , the deficiencies over the ocean for the C
12 and PW categorizations are absent for each.

13 The ModelE δD changes in δD underfor the categorical operators result from approximating the controls
14 on retrieval quality and p_D using conditions in the model, rather than from collocated TES retrievals. They
15 are accurate to the extent that the approximated controls in Fig. 11 and Fig. 13 agree with the
16 observational controls in Fig. 4. Focusing on the full LOCTPW categorization, the most significant
17 deficiency was the PW_F control on p_D over the ocean (Fig. 13d), where the approximated slope was -1.6
18 hPa/mm too strong compared to observations. We can see, however, that while the slope for the
19 LO τ TPW $_F$ categorization was only -1.2 hPa/mm too strong, this translated into less than a 1 ‰ difference
20 in the mean change in δD over the ocean from the LOCPTW categorization (Fig. 15 c, d). This suggests
21 that if a categorization existed that more closely approximated the observed PW_F control on p_D in the
22 observations, this would not likely result in change of more than several ‰ to the transformed δD field,
23 ignoring the contributions of other secondary controls. This provides a sense of the maximum error in the
24 transformed δD field associated with errors in quality filtering and averaging kernel selection. We note
25 also that in this case, the change in δD for the retrieval-based and LOCTPW categorical operator were

1 very similar, owing to the agreement in the underlying PW_F fields, and because of the shared HDO prior
2 and raw model δD fields.

3 **6.2 Sensitivity tests**

4 To further understand how the change in δD might vary with different configurations, we examined the
5 sensitivity of the LOCTPW-based operator to the effects of orbital sampling, a fixed H₂O prior \mathbf{x}_a^H , and
6 also the performance outside of the tropics.

7 The effect of sampling the model at all points and not just along the TES orbital path was primarily a
8 smoother transformed field (Fig. 16a) compared to without (Fig. 15e) owing to a much greater sampling
9 frequency. Aghedo et al. (2011) found that the effects of orbital path sampling were also minimal on
10 modeled CO, O₃, temperature and H₂O at a monthly scale. Voulgarakis et al. (2011) also reached to a
11 similar conclusion regarding the correlation between daily O₃ and CO. The TES sampling frequency is
12 therefore sufficient to capture variability in the model over several years, although it remains to be seen
13 whether this is the case at shorter time scales.

14 | Unique to the joint TES HDO/H₂O retrievals is the use of a changing H₂O prior \mathbf{x}_a^H . It must also be
15 | chosen in applying the TES operator, representing another potential source of categorical selection error.
16 We assume that the quality of averaging kernel selection for the A_{HH} , A_{DH} and A_{HD} operators for different
17 | categorizations follows that of A_{DD} . As a test of the importance of \mathbf{x}_a^H selection on the TES operator in
18 | Eq. (1), we fixed \mathbf{x}_a^H to the constant profile of the ‘Single’ categorization, but with the averaging kernels
19 | still chosen from the LOCTPW categorization. This had little effect (Fig. 16b), which likely means that
20 the A_{HH} and A_{DH} terms are typically very similar (as was the case for the example profile in Fig. 2), and
21 that the strength of TES operator is largely controlled by the second term on the RHS of Eq. (1).

22 The focus of future comparisons between the modeled and observed δD fields will be over the tropics,
23 following a series of recent studies (Lee et al., 2011; Kurita et al., 2011; Berkelhammer et al., 2012; Kim
24 et al., in press). For broader potential application, however, we tested the performance of the TES HDO

1 simulator outside of the tropical domain. The LOCTPW categorization was re-calculated from TES
2 measurements over 60°S to 60°N. The range of the surface temperature categories was increased from
3 260K to 330K to capture a wider observed temperature range. Model simulations were run with the TES
4 operators applied over 60°S to 60°N. To assess performance outside of the tropics, we examine the degree
5 to which observed variation in relationship strength by latitude is captured by the categorical TES
6 operator.

7 Fig. 17 shows the correlation between retrieval quality and p_D and the primary control variables at
8 different latitudes. Observed retrieval quality over the oceans (Fig. 17a) remains negatively correlated
9 with CF , weakening slightly at high northern latitudes. The retrieval-based operator performs poorly in
10 capturing this association, but the categorical operator performs well. Over land (Fig. 17c), the observed
11 negative correlation between retrieval quality and T_S becomes positive at high latitudes, presumably due
12 to the covariation moving poleward between T_S and atmospheric moisture content. This change is
13 captured by both operators, but too sharply in the case of the categorical operator.

14 The associations between p_D and the primary control variables are not generally well-captured over the
15 wider latitude range. Over the ocean (Fig. 17b), the overly-strong negative correlation between p_D and
16 PW_F over the tropics compared to observations (in Table1) increases moving poleward. The observed
17 decrease in correlation outside of the tropics is captured to some degree by the categorical operator, but
18 with a lag, and nor is there any modeled rebound in correlation at high latitudes. Over land, there is an
19 observed positive relationship between T_S and p_D across all latitudes (Figure 2d). This is poorly captured
20 by the categorical operator, for which there is no correlation between 40°S and 0°. In fact, over land,
21 when extratropical TES measurements are included in calculating the categorization, the performance of
22 the operator is degraded in the tropics. When the categorization is calculated only from TES
23 measurements between 15S and 15N, the correlation between p_D and T_S of 0.64 is in good agreement
24 with the observed correlation of 0.51. When the operator is based on measurements between 60S to 60N,
25 however, the correlation over 15S to 15N is 0.00. So not only is prediction of p_D in the extra tropics poor,

1 but it contaminates the fairly good performance over the tropical land shown in Fig. 13j. Application of
2 the categorical TES operator outside of the tropics will likely require that latitude-specific categorizations
3 be computed from the TES retrievals, and possibly that other control variables be considered.

4 **6.3 Comparison with TES δD**

5 Comparisons between the TES and ModelE δD are shown in Fig. 18. The raw ModelE δD is on average
6 17 ‰ lower than TES over the ocean and 41 ‰ lower than TES over land, but with negative biases of up
7 to 63 ‰ and 96 ‰ over each, respectively (Fig. 18b). The negative bias over the ocean occurs over the
8 tropical rain bands and in the dry regions off of the west South American and central African coasts. In
9 the latter cases, the bias likely results from outflow of strongly depleted vapor due to continental
10 convection.

11 The negative bias over the ocean is reduced to ~ 7 ‰ after applying either the retrieval-based (Fig. 18c) or
12 categorical (Fig. 18d) TES operators, and more weakly reduced to ~ 35 ‰ over land. The changes in bias
13 over the ocean are interpreted as follows. Where there is heavy, precipitating cloud, observed retrieval
14 quality is lower (Fig. 3a). Because precipitation tends to lower vapor δD (e.g. Lee and Fung, 2008), this
15 introduces an observational bias toward higher δD through the exclusion of retrievals under cloudy and
16 lower δD conditions, and relaxation toward a prior constraint with higher δD . By applying the TES
17 operator, these effects are captured (Fig. 14c, Fig. 15e) leading to the more accurate comparisons in Fig.
18 18 c,d. It also becomes more apparent that the model bias toward lower δD is specific to a model process
19 over land. It was beyond the scope of this paper to understand these biases, but immediate candidates that
20 will be investigated in the future are too-strong continental convection and too-weak transpiration.

21 **7. Discussion**

22 Changes to the raw model δD over the tropics from applying the TES operators were large. Over the
23 ocean, the mean increase in modeled δD from applying the TES operator was 9 ‰, and was up to 30 ‰

1 over regions with low, raw δD such as the west Pacific warm pool. Over land, there was a mean increase
2 of 6 ‰, but with increases of up to 30 ‰, and decreases of up to 40 ‰ over northeastern Africa where
3 raw δD is very high.

4 To put these changes in context, they are of the same order as the δD model biases in previous
5 comparisons against the TES δD retrievals. Yoshimura et al. (2011) saw a systematic bias of -20 ‰ in the
6 IsoGSM model over the same vertical layer. Risi et al. (2012) saw a bias of 30 ‰ in their comparison of
7 LMDz at 619 hPa. That the regional differences to the raw ModelE δD fields resulting from the TES
8 operator are of the same magnitude confirm its importance in any quantitative comparison between the
9 model and satellite measurements. Similarly, Aghedo et al. (2011) determined that the error associated
10 with not applying the TES retrieval operator to retrieved CO, O₃, temperature, and particularly H₂O, was
11 much larger than the error associated with monthly averaging or the absence of orbital sampling.

12 The changes in δD for the cloud-only categorization were unrealistic owing to poor p_D approximation.
13 For this nudged simulation, the new δD fields for retrieval-based and full LOCTPW categorical operators
14 were in good agreement because of the similarity of their PW_F and T_S fields and because of accurate
15 mapping of these quantities to a suitable averaging kernel. The LO τ PW_F categorization generally
16 performed well through its inclusion of the most important controls on retrieval quality and p_D , and has
17 the advantage of having far fewer categories, but the influence of T_S on p_D over land was too strong. The
18 accuracy of the modeled PW_F field is likely the result of the nudged, large-scale control on the humidity
19 field and averaging over four years. It is doubtful that this agreement will be the case for free-running
20 simulations with strongly perturbed physics or over shorter time scales, in which case the categorical
21 operator would be more appropriate.

22 Particularly for retrieval quality, the categorical operator performed poorly over land compared to the
23 ocean. One factor is simply that estimates of categorical retrieval quality averaging kernel structure over
24 land will be less robust because there are fewer TES measurements. More importantly is that there are

1 likely additional factors influencing retrieval quality and averaging kernel structure over land that we
2 have not considered. For p_D in particular, the observational controls over land were weaker (Table1),
3 making their approximation in the simulator more difficult. As the categorical operator evolves, we will
4 start by testing topography, land cover type, and, related to both, thermal contrast between ground and air,
5 which will be greater over land than ocean. In the latter case, the apparently worse performance over land
6 could be because we considered daytime retrievals only.

7 Further refinements will be required to use the categorical operator outside of the tropics. Over the
8 oceans, more PW_B and PW_F categories will be required at the low ends of their scales, assuming that
9 vertical moisture gradients continue to be the dominant control on p_D outside of the tropics. Any
10 improvements that are obtained over land in the tropics should improve performance in the extratropics,
11 particularly in the northern hemisphere. We hope to avoid computing the categorizations separately for
12 different latitude bands, but this might be inevitable.

13 ~~In that context, isotopic~~ isotopic constraints provide a new way of assessing GCM simulations of
14 processes which are highly sensitive to perturbed cloud physics, such as those driving the Madden-Julian
15 Oscillation (MJO). Berkelhammer et al. (2012) separated the contributions of evaporative and convergent
16 moisture phases during different phases of the MJO. Kim et al. (in press) showed how the absence of an
17 MJO in the default AR5 version of ModelE could be rectified by increasing the entrainment and
18 reevaporation strength in the convective parameterization, but at the expense of the mean state of
19 precipitation. It would be instructive to compare the isotopic response of these changes to TES HDO
20 retrievals, given the sensitivity of isotopic composition to these types of processes (Worden et al., 2007b;
21 Lee et al., 2009; Field et al., 2010). The categorical TES operator provides a means of doing this for
22 arbitrary convective configurations, ~~although further refinements will be required for studies outside of~~
23 ~~the tropics.~~

1 In comparisons between retrieved and simulated HDO for other models, regardless of which operator
2 approach is taken, or some other approach, we suggest looking at the agreement between retrieved and
3 modeled CF , PW_F and T_S . This will give a sense of how appropriate the retrieval quality filtering and
4 averaging kernel selection is for the modeled meteorology, particularly as observational constraints are
5 weakened with free-running perturbed physics experiments. It remains to be seen how the categorical
6 approach performs for free-running model simulations or for other isotopically-equipped AGCMs. The
7 modeled retrieval quality and p_D fields (i.e. in Fig. 10 and Fig. 12) will change to the extent that the
8 underlying control fields change, or rather, to the extent that the covariation between the control variables
9 changes. One potential weakness is that a new model configuration will have an increase in the frequency
10 of conditions corresponding to categories that were not well populated by TES measurements and for
11 which the retrieval quality and mean averaging kernels are less robust (although the opposite could also
12 be true). This type of evaluation could also be extended to other species, such as O_3 and CO , after
13 identifying the strongest controls on their retrieval quality and averaging kernel structure, as could the
14 categorical TES operator for use in non-nudged composition-climate model evaluation. We note that
15 cloud cover and surface temperature will likely play an important role for most species, but the
16 importance of atmospheric moisture content is likely specific to HDO.

18 **Acknowledgements**

19 RF was supported by the NASA Postdoctoral Program, CR by NASA grant NNX08AR23G, GS and JW
20 by the NASA Energy and Water Cycle Study grant 07-NEWS07-20, ~~and~~ AV by the Atmospheric
21 Chemistry Modeling and Analysis Program, and AS by NASA grant NNX09AK34G-. Part of this
22 research was carried out at the Jet Propulsion Laboratory, California Institute of Technology, under a
23 contract with the National Aeronautics and Space Administration. Resources supporting this work were
24 provided by the NASA High-End Computing (HEC) Program through the NASA Center for Climate
25 Simulation (NCCS) at Goddard Space Flight Center.

1 **References**

- 2 Aghedo, A. M., Bowman, K. W., Worden, H. M., Kulawik, S. S., Shindell, D. T., Lamarque, J. F.,
3 Faluvegi, G., Parrington, M., Jones, D. B. A., and Rast, S.: The vertical distribution of ozone
4 instantaneous radiative forcing from satellite and chemistry climate models, *J Geophys Res-*
5 *Atmos*, 116, D01305, doi: 10.1029/2010jd014243, 2011.
- 6 Bacmeister, J. T., Suarez, M. J., and Robertson, F. R.: Rain reevaporation, boundary layer-convection
7 interactions, and Pacific rainfall patterns in an AGCM, *Journal of the Atmospheric Sciences*, 63,
8 3383-3403, 2006.
- 9 Beer, R., Glavich, T. A., and Rider, D. M.: Tropospheric emission spectrometer for the Earth Observing
10 System's Aura Satellite, *Applied Optics*, 40, 2356-2367, 2001.
- 11 Berkelhammer, M., Risi, C., Kurita, N., and Noone, D. C.: The moisture source sequence for the Madden-
12 Julian Oscillation as derived from satellite retrievals of HDO and H2O, *J Geophys Res-Atmos*,
13 117, [D03106](https://doi.org/10.1029/2011JD016803), doi:10.1029/2011JD016803, 2012.
- 14 Bodas-Salcedo, A., Webb, M. J., Bony, S., Chepfer, H., Dufresne, J. L., Klein, S. A., Zhang, Y.,
15 Marchand, R., Haynes, J. M., Pincus, R., and John, V. O.: COSP Satellite simulation software for
16 model assessment, *Bulletin of the American Meteorological Society*, 92, 1023-1043, Doi
17 10.1175/2011bams2856.1, 2011.
- 18 Choi, Y., Osterman, G., Eldering, A., Wang, Y. H., and Edgerton, E.: Understanding the contributions of
19 anthropogenic and biogenic sources to CO enhancements and outflow observed over North
20 America and the western Atlantic Ocean by TES and MOPITT, *Atmospheric Environment*, 44,
21 2033-2042, DOI 10.1016/j.atmosenv.2010.01.029, 2010.
- 22 Clough, S. A., Shephard, M. W., Worden, J., Brown, P. D., Worden, H. M., Luo, M., Rodgers, C. D.,
23 Rinsland, C. P., Goldman, A., Brown, L., Kulawik, S. S., Eldering, A., Lampel, M., Osterman,

1 G., Beer, R., Bowman, K., Cady-Pereira, K. E., and Mlawer, E. J.: Forward model and Jacobians
2 for Tropospheric Emission Spectrometer retrievals, IEEE Trans. Geosci. Remote Sensing, 44,
3 1308-1323, Doi 10.1109/Tgrs.2005.860986, 2006.

4 [Eldering, A., S. S. Kulawik, J. Worden, K. Bowman, and G. Osterman \(2008\), Implementation of cloud](#)
5 [retrievals for TES atmospheric retrievals: 2. Characterization of cloud top pressure and effective](#)
6 [optical depth retrievals, *J. Geophys. Res.-Atmos.*, 113\(D16\), D16D37, doi:](#)
7 [10.1029/2007jd008858.](#)

8 Field, R. D., Jones, D. B. A., and Brown, D. P.: Effects of postcondensation exchange on the isotopic
9 composition of water in the atmosphere, J Geophys Res-Atmos, 115, doi:10.1029/2010jd014334,
10 D24305, doi:10.1029/2010jd014334, 2010.

11 Jones, D. B. A., Bowman, K. W., Palmer, P. I., Worden, J. R., Jacob, D. J., Hoffman, R. N., Bey, I., and
12 Yantosca, R. M.: Potential of observations from the Tropospheric Emission Spectrometer to
13 constrain continental sources of carbon monoxide, J Geophys Res-Atmos, 108,
14 doi:10.1029/2003jd003702, 4789, doi:10.1029/2003jd003702, 2003.

15 Jones, D. B. A., Bowman, K. W., Logan, J. A., Heald, C. L., Liu, J., Luo, M., Worden, J., and
16 Drummond, J.: The zonal structure of tropical O(3) and CO as observed by the Tropospheric
17 Emission Spectrometer in November 2004-Part 1: Inverse modeling of CO emissions,
18 Atmospheric Chemistry and Physics, 9, 3547-3562, 2009.

19 Kalnay, E., Kanamitsu, M., Kistler, R., Collins, W., Deaven, D., Gandin, L., Iredell, M., Saha, S., White,
20 G., Woollen, J., Zhu, Y., Chelliah, M., Ebisuzaki, W., Higgins, W., Janowiak, J., Mo, K. C.,
21 Ropelewski, C., Wang, J., Leetmaa, A., Reynolds, R., Jenne, R., and Joseph, D.: The
22 NCEP/NCAR 40-Year Reanalysis Project, Bulletin of the American Meteorological Society, 77,
23 437-471, 1996.

- 1 Kim, D., Del Genio, A. D., and Yao, M. S.: Moist convection scheme in Model E2, NASA Goddard
2 Institute for Space Studies, New York, 2011.
- 3 Kim, D., Sobel, A. H., Del Genio, A., Chen, Y.-H., Camargo, S. J., Yao, M.-S., Kelley, M., and
4 Nazarenko, L.: The Tropical Subseasonal Variability Simulated in the NASA GISS General
5 Circulation Model, *Journal of Climate*, in press, doi:10.1175/JCLI-D-11-00447.1., [4641–4659](#),
6 2012.
- 7 Klein, S. A., and Jakob, C.: Validation and sensitivities of frontal clouds simulated by the ECMWF
8 model, *Monthly Weather Review*, 127, 2514-2531, 1999.
- 9 Kurita, N., Noone, D., Risi, C., Schmidt, G. A., Yamada, H., and Yoneyama, K.: Intraseasonal isotopic
10 variation associated with the Madden-Julian Oscillation, *J Geophys Res-Atmos*, 116, D24101,
11 doi: 10.1029/2010jd015209, 2011.
- 12 Lee, J. E., and Fung, I.: "Amount effect" of water isotopes and quantitative analysis of post-condensation
13 processes, *Hydrol. Process.*, 22, 1-8, doi: 10.1002/Hyp.6637, 2008.
- 14 Lee, J. E., Pierrehumbert, R., Swann, A., and Lintner, B. R.: Sensitivity of stable water isotopic values to
15 convective parameterization schemes, *Geophysical Research Letters*, 36,
16 doi:10.1029/2009gl040880, L23801, doi: 10.1029/2009gl040880, 2009.
- 17 Lee, J., Worden, J., Noone, D., Bowman, K., Eldering, A., LeGrande, A., Li, J. L. F., Schmidt, G., and
18 Sodemann, H.: Relating tropical ocean clouds to moist processes using water vapor isotope
19 measurements, *Atmospheric Chemistry and Physics*, 11, 741-752, 10.5194/acp-11-741-2011,
20 2011.
- 21 Liu, J. J., Jones, D. B. A., Worden, J. R., Noone, D., Parrington, M., and Kar, J.: Analysis of the
22 summertime buildup of tropospheric ozone abundances over the Middle East and North Africa as

1 observed by the Tropospheric Emission Spectrometer instrument, J Geophys Res-Atmos, 114,
2 doi: 10.1029/2008jd010993, D05304, doi: 10.1029/2008jd010993, 2009.

3 Luo, M., Rinsland, C., Fisher, B., Sachse, G., Diskin, G., Logan, J., Worden, H., Kulawik, S., Osterman,
4 G., Eldering, A., Herman, R., and Shephard, M.: TES carbon monoxide validation with DACOM
5 aircraft measurements during INTEX-B 2006, J Geophys Res-Atmos, 112,
6 doi:10.1029/2007jd008803, D24S48, doi:10.1029/2007jd008803, 2007a.

7 Luo, M., Rinsland, C. P., Rodgers, C. D., Logan, J. A., Worden, H., Kulawik, S., Eldering, A., Goldman,
8 A., Shephard, M. W., Gunson, M., and Lampel, M.: Comparison of carbon monoxide
9 measurements by TES and MOPITT: Influence of a priori data and instrument characteristics on
10 nadir atmospheric species retrievals, J Geophys Res-Atmos, 112, D09303,
11 doi:10.1029/2006jd007663, 2007b.

12 Nassar, R., Logan, J. A., Worden, H. M., Megretskaia, I. A., Bowman, K. W., Osterman, G. B.,
13 Thompson, A. M., Tarasick, D. W., Austin, S., Claude, H., Dubey, M. K., Hocking, W. K.,
14 Johnson, B. J., Joseph, E., Merrill, J., Morris, G. A., Newchurch, M., Oltmans, S. J., Posny, F.,
15 Schmidlin, F. J., Vomel, H., Whiteman, D. N., and Witte, J. C.: Validation of Tropospheric
16 Emission Spectrometer (TES) nadir ozone profiles using ozonesonde measurements, J Geophys
17 Res-Atmos, 113, doi:10.1029/2007jd008819, D15S17, doi:10.1029/2007jd008819, 2008.

18 Nassar, R., Logan, J. A., Megretskaia, I. A., Murray, L. T., Zhang, L., and Jones, D. B. A.: Analysis of
19 tropical tropospheric ozone, carbon monoxide, and water vapor during the 2006 El Nino using
20 TES observations and the GEOS-Chem model, J Geophys Res-Atmos, 114, D17304, doi:
21 10.1029/2009jd011760, 2009.

22 Nassar, R., Jones, D. B. A., Kulawik, S. S., Worden, J. R., Bowman, K. W., Andres, R. J.,
23 Suntharalingam, P., Chen, J. M., Brenninkmeijer, C. A. M., Schuck, T. J., Conway, T. J., and
24 Worthy, D. E.: Inverse modeling of CO(2) sources and sinks using satellite observations of CO(2)

1 from TES and surface flask measurements, Atmospheric Chemistry and Physics, 11, 6029-6047,
2 10.5194/acp-11-6029-2011, 2011.

3 Norris, P. M., and Da Silva, A. M.: Assimilation of satellite cloud data into the GMAO finite-volume data
4 assimilation system using a parameter estimation method. Part I: Motivation and algorithm
5 description, Journal of the Atmospheric Sciences, 64, 3880-3895, Doi 10.1175/2006jas2046.1,
6 2007.

7 Parrington, M., Jones, D. B. A., Bowman, K. W., Horowitz, L. W., Thompson, A. M., Tarasick, D. W.,
8 and Witte, J. C.: Estimating the summertime tropospheric ozone distribution over North America
9 through assimilation of observations from the Tropospheric Emission Spectrometer, J Geophys
10 Res-Atmos, 113, doi:10.1029/2007jd009341, D18307, doi: 10.1029/2007jd009341, 2008.

11 Prather, M. J.: Numerical Advection by Conservation of 2nd-Order Moments, J Geophys Res-Atmos, 91,
12 6671-6681, 1986.

13 Rayner, N. A., Parker, D. E., Horton, E. B., Folland, C. K., Alexander, L. V., Rowell, D. P., Kent, E. C.,
14 and Kaplan, A.: Global analyses of sea surface temperature, sea ice, and night marine air
15 temperature since the late nineteenth century, J Geophys Res-Atmos, 108,
16 doi:10.1029/2002jd002670, 4407, doi:10.1029/2002jd002670, 2003.

17 Richards, N. A. D., Osterman, G. B., Browell, E. V., Hair, J. W., Avery, M., and Li, Q. B.: Validation of
18 Tropospheric Emission Spectrometer ozone profiles with aircraft observations during the
19 intercontinental chemical transport experiment-B, J Geophys Res-Atmos, 113,
20 doi:10.1029/2007jd008815, D16S29, doi: 10.1029/2007jd008815, 2008.

21 Rienecker, M., Suarez, M., Todling, R., Bacmeister, J., Takacs, L., Liu, H., Gu, W., Sienkiewicz, M.,
22 Koster, R., Gelaro, R., Stajner, I., and Nielsen, E.: The GEOS-5 Data Assimilation System -
23 Documentation of Versions 5.0.1, 5.1.0, and 5.2.0, NASA/TM-2007-104606, 2007.

1 Rinsland, C. P., Luo, M., Shephard, M. W., Clerbaux, C., Boone, C. D., Bernath, P. F., Chiou, L., and
2 Coheur, P. F.: Tropospheric emission spectrometer (TES) and atmospheric chemistry experiment
3 (ACE) measurements of tropospheric chemistry in tropical southeast Asia during a moderate El
4 Nino in 2006, *J. Quant. Spectrosc. Radiat. Transf.*, 109, 1931-1942, 10.1016/j.jqsrt.2007.12.020,
5 2008.

6 Risi, C., Noone, D., Worden, J., Frankenberg, C., Stiller, G., Kiefer, M., Funke, B., Walker, K., Bernath,
7 P., Schneider, M., Wunch, D., Sherlock, V., Deutscher, N., Griffith, D., Wennberg, P. O., Strong,
8 K., Smale, D., Mahieu, E., Barthlott, S., Hase, F., García, O., Notholt, J., Warneke, T., Toon, G.,
9 Sayres, D., Bony, S., Lee, J., Brown, D., Uemura, R., and Sturm, C.: Process-evaluation of
10 tropospheric humidity simulated by general circulation models using water vapor isotopologues:
11 1. Comparison between models and observations, *J. Geophys. Res.*, 117, D05303,
12 10.1029/2011jd016621, 2012.

13 Schmidt, G. A., Hoffmann, G., Shindell, D. T., and Hu, Y. Y.: Modeling Atmospheric Stable Water
14 Isotopes and the Potential for Constraining Cloud Processes and Stratosphere-Troposphere Water
15 Exchange, *J Geophys Res-Atmos*, 110, doi: 10.1029/2005jd005790, D21314, doi:
16 10.1029/2005jd005790, 2005.

17 Schmidt, G. A., Ruedy, R., Hansen, J. E., Aleinov, I., Bell, N., Bauer, M., Bauer, S., Cairns, B., Canuto,
18 V., Cheng, Y., Del Genio, A., Faluvegi, G., Friend, A. D., Hall, T. M., Hu, Y. Y., Kelley, M.,
19 Kiang, N. Y., Koch, D., Lacis, A. A., Lerner, J., Lo, K. K., Miller, R. L., Nazarenko, L., Oinas,
20 V., Perlwitz, J., Perlwitz, J., Rind, D., Romanou, A., Russell, G. L., Sato, M., Shindell, D. T.,
21 Stone, P. H., Sun, S., Tausnev, N., Thresher, D., and Yao, M. S.: Present-Day Atmospheric
22 Simulations Using GISS ModelE: Comparison to in Situ, Satellite, and Reanalysis Data, *Journal*
23 *of Climate*, 19, 153-192, 2006.

1 Sherwood, S. C., Roca, R., Weckwerth, T. M., and Andronova, N. G.: Tropospheric Water Vapor,
2 Convection, and Climate, *Reviews of Geophysics*, 48, doi:10.1029/2009rg000301, ~~Attn~~
3 ~~Rg2004RG2001~~, ~~Doi~~-doi: 10.1029/2009rg000301, 2010.

4 Voulgarakis, A., Telford, P. J., Aghedo, A. M., Braesicke, P., Faluvegi, G., Abraham, N. L., Bowman, K.
5 W., Pyle, J. A., and Shindell, D. T.: Global multi-year O(3)-CO correlation patterns from models
6 and TES satellite observations, *Atmospheric Chemistry and Physics*, 11, 5819-5838,
7 10.5194/acp-11-5819-2011, 2011.

8 Worden, J., Bowman, K., Noone, D., Beer, R., Clough, S., Eldering, A., Fisher, B., Goldman, A., Gunson,
9 M., Herman, R., Kulawik, S. S., Lampel, M., Luo, M., Osterman, G., Rinsland, C., Rodgers, C.,
10 Sander, S., Shephard, M., and Worden, H.: Tropospheric emission spectrometer observations of
11 the tropospheric HDO/H₂O ratio: Estimation approach and characterization, *J Geophys Res-*
12 *Atmos*, 111, doi: 10.1029/2005jd006606, D16309, doi: 10.1029/2005jd006606, 2006.

13 Worden, H. M., Logan, J. A., Worden, J. R., Beer, R., Bowman, K., Clough, S. A., Eldering, A., Fisher,
14 B. M., Gunson, M. R., Herman, R. L., Kulawik, S. S., Lampel, M. C., Luo, M., Megretskaia, I.
15 A., Osterman, G. B., and Shephard, M. W.: Comparisons of Tropospheric Emission Spectrometer
16 (TES) ozone profiles to ozonesondes: Methods and initial results, *J Geophys Res-Atmos*, 112,
17 10.1029/2006jd007258, D03309, doi: 10.1029/2006jd007258, 2007a.

18 Worden, J., Noone, D., and Bowman, K.: Importance of Rain Evaporation and Continental Convection in
19 the Tropical Water Cycle, *Nature*, 445, 528-532, 2007b.

20 Worden, J., Noone, D., Galewsky, J., Bailey, A., Bowman, K., Brown, D., Hurley, J., Kulawik, S., Lee,
21 J., and Strong, M.: Estimate of bias in Aura TES HDO/H₂O profiles from comparison of TES
22 and in situ HDO/H₂O measurements at the Mauna Loa observatory, *Atmospheric Chemistry*
23 *and Physics*, 11, 4491-4503, doi: 10.5194/acp-11-4491-2011, 2011.

1 Yoshimura, K., Frankenberg, C., Lee, J., Kanamitsu, M., Worden, J., and Rockmann, T.: Comparison of
2 an isotopic atmospheric general circulation model with new quasi-global satellite measurements
3 of water vapor isotopologues, *J Geophys Res-Atmos*, 116, D19118, doi:10.1029/2011jd016035,
4 2011.

1 **Tables**

2 **Table 1. Pattern correlation between TES HDO retrieval quality (Fig. 3a) and p_D (height of peak HDO averaging kernel sensitivity) (Fig. 3b) and candidate variables.**
 3 **Cloud fraction is the frequency of occurrence within a grid cell of observations with τ greater than 0.3. For p_D , correlations are for high-quality observations only. The**
 4 **strongest correlation in for each column is shown in bold.**

Description	Variable	Retrieval quality		Pressure of peak HDO sensitivity (p_D)	
		Ocean	Land	Ocean	Land
Cloud optical depth	τ	-0.38	0.30	-0.39	-0.35
Cloud fraction (%)	CF	-0.70	0.39	-0.55	-0.28
Cloud top pressure (hPa)	CTP	0.33	0.15	0.13	0.00
Prep. water in bdy. layer (mm)	PW_B	-0.15	0.57	-0.29	-0.39
Prep. water in free. atm. (mm)	PW_F	-0.43	0.32	-0.70	-0.50
Prep. water total (mm)	PW_T	-0.35	0.44	-0.58	-0.48
Surface temperature (K)	T_S	-0.28	-0.72	0.04	0.51

1

2 **Table 2. Category values for different parameters.**

Identifier	Description	Category ranges
LO	Land / ocean	
C	τ	0, 0.3, 1.3, 3.6, 23, > 23
	<i>CTP</i> (hPa)	0, 440, 680, > 680
C_fine	τ	0, 0.3, 1.3, 3.6, 9.4, 23, 60, > 60
	<i>CTP</i> (hPa)	0, 180, 310, 440, 560, 680, 800, > 800
T	T_S (K)	< 295, 295, 300, 305, 310, 315, > 315
PW	PW_B, PW_F (mm)	0, 10, 20, > 20
PW_fine	PW_B, PW_F (mm)	0, 5, 10, 15, 20, 25, 30, > 30

3

4

1 **Table 3. Frequency of occurrence (%) for TES retrievals for the C categorization. There was a total of 202 713 retrievals**
 2 **during daytime over the tropics.**

		Cloud optical depth				
		0 -0.3	0.3 - 1.3	1.3 - 3.6	3.6 - 23	> 23
Cloud top	0 - 440	43.3	7.3	4.1	5.8	0
pressure	440 - 680	17.2	4.2	5.6	1.6	0
(hPa)	680 - 1000	3.5	2	2.5	2	0.8

3

1 **Table 4. Percentage of TES retrievals that were high quality for the C categorization. Overall, 69% of retrievals were**
 2 **high quality.**

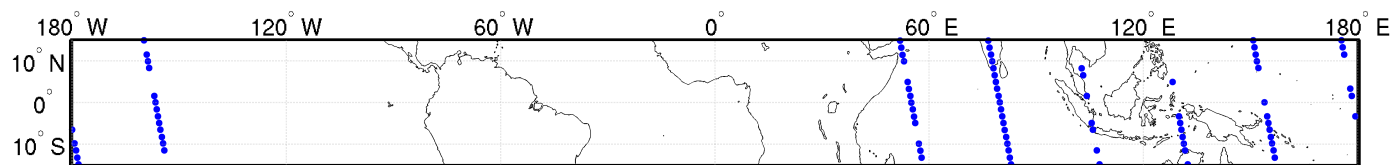
		Cloud optical depth				
		0 - 0.3	0.3 - 1.3	1.3 - 3.6	3.6 - 23	> 23
Cloud top pressure (hPa)	0 - 440	79	86.1	11.6	0	
	440 - 680	78.8	85.5	39	10.4	
	680 - 1000	68.2	81	83.1	64.4	26.8

3

4

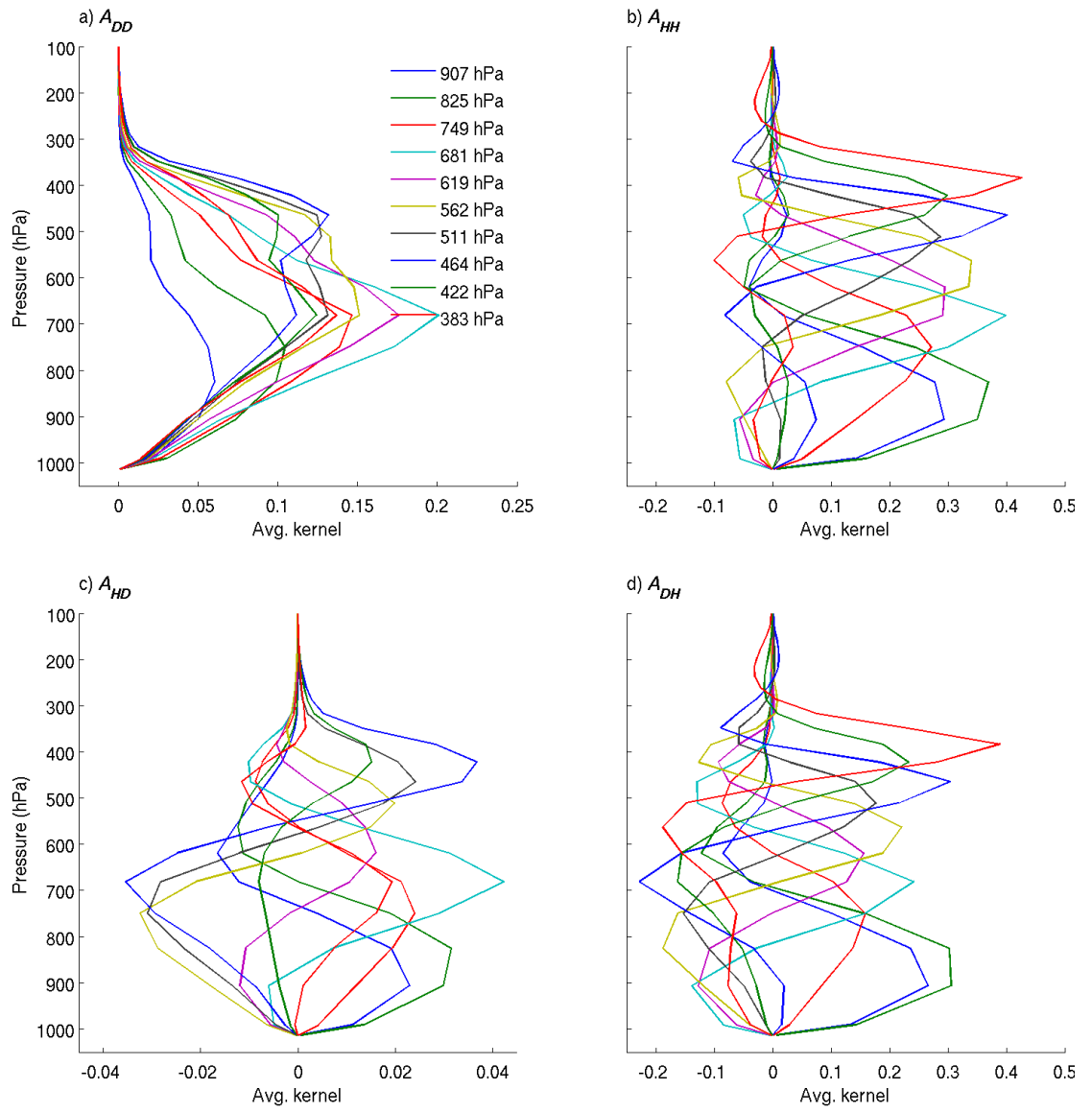
1 **Figures**

2
3



4

5 **Fig. 1.** Aura TES nadir orbit for December 9, 2006 during daytime over 15°S to 15°N. Only the 85 high quality HDO retrievals are shown, of 133 in total.

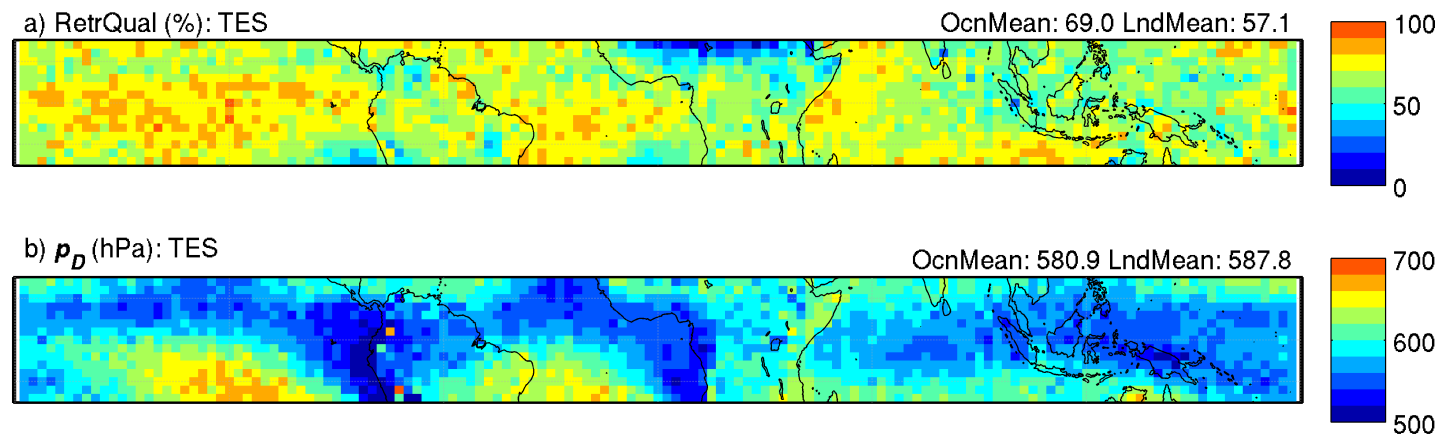


1

2

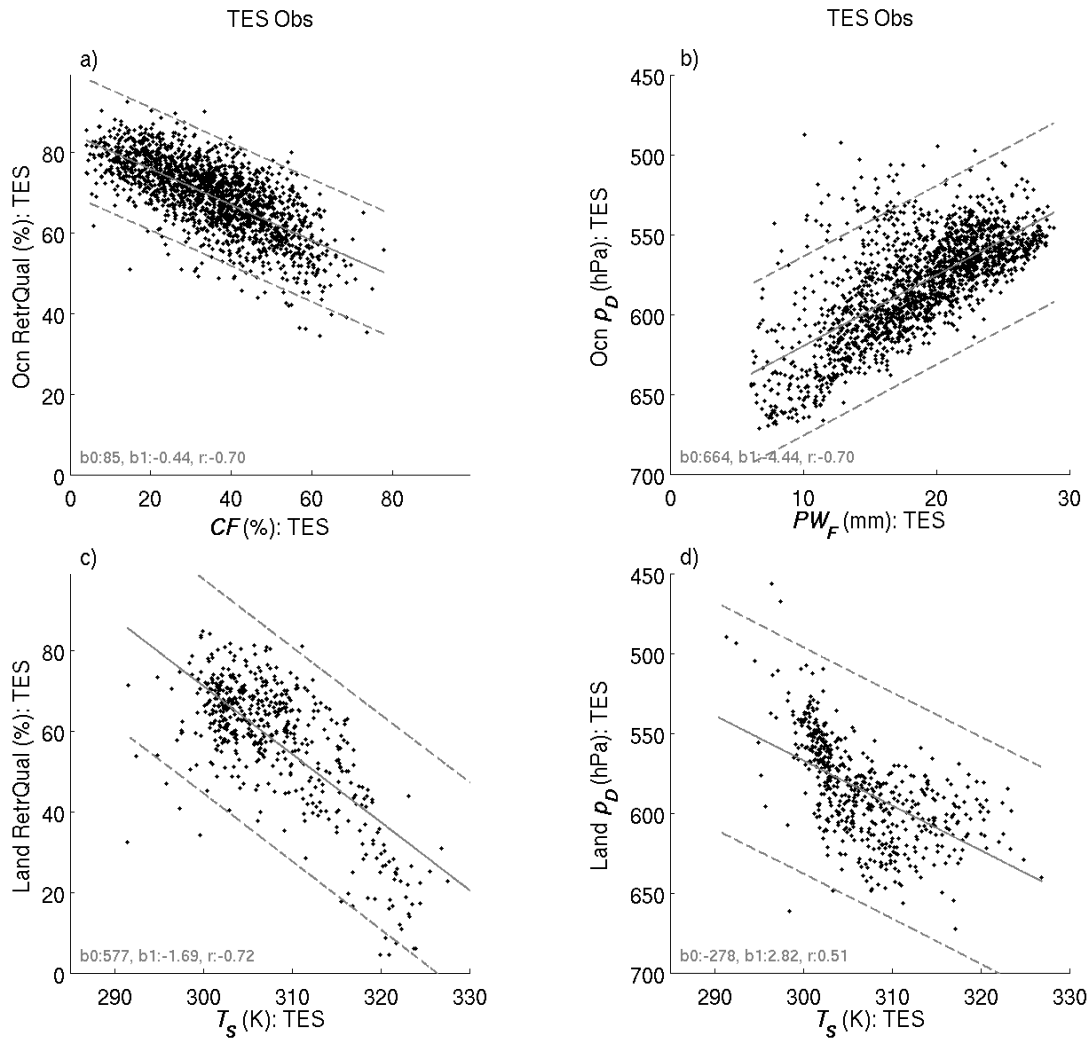
3 **Fig. 2. Averaging kernels for the retrieval at 10:00 UTC, December 9, 2006 at (3.0N, 53.75E).**

1



2

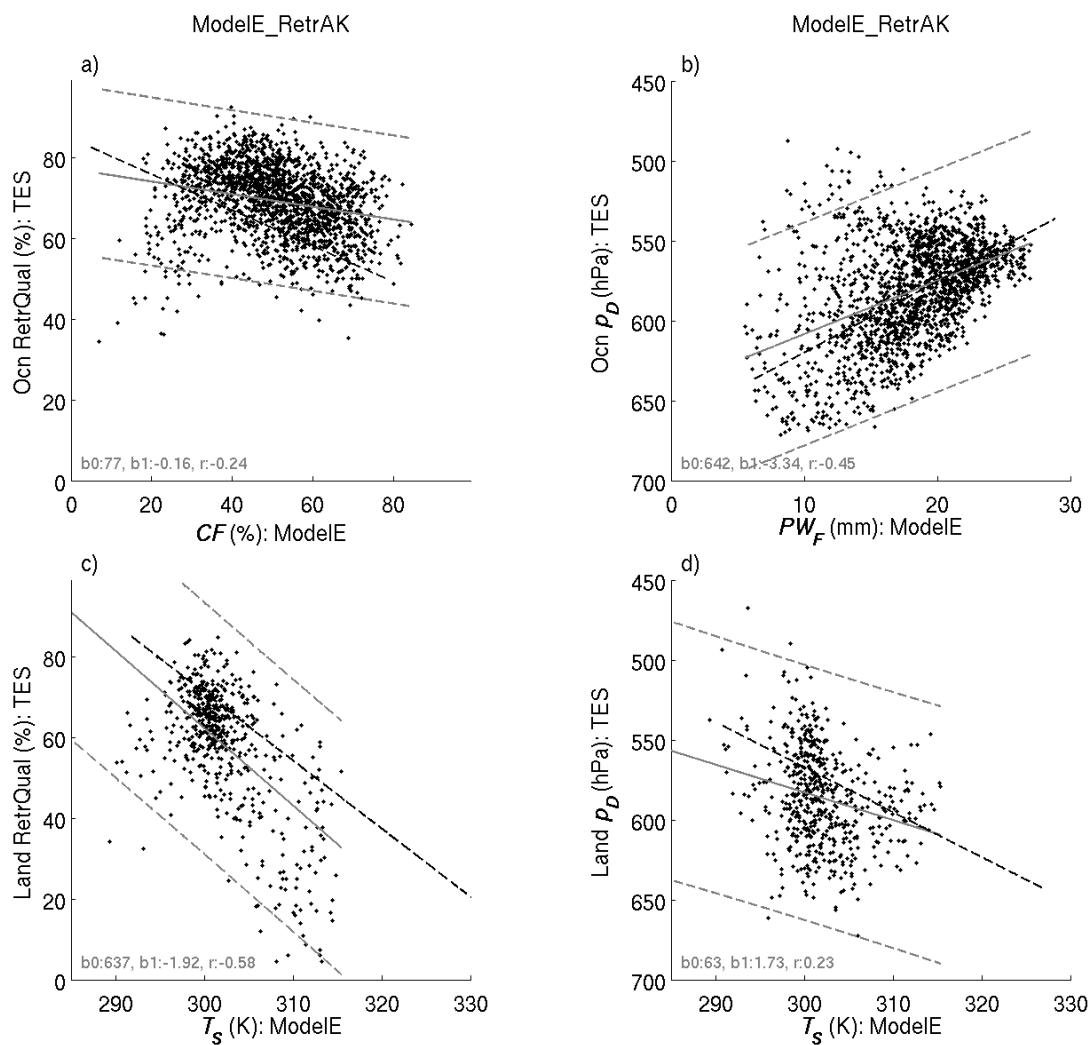
3 Fig. 3. a) TES HDO retrieval quality and b) mean p_D (height of peak HDO sensitivity) over 825 to 510 hPa for high quality retrievals only. Both fields are the mean
4 across all retrievals from 2006-2009.



1

2 **Fig. 4. TES retrieval quality (left) and p_D (height of peak HDO sensitivity, right) as a function of primary control**
 3 **variables identified in Table 1 over ocean (top) and land (bottom). Dashed lines show the 95% prediction intervals.**

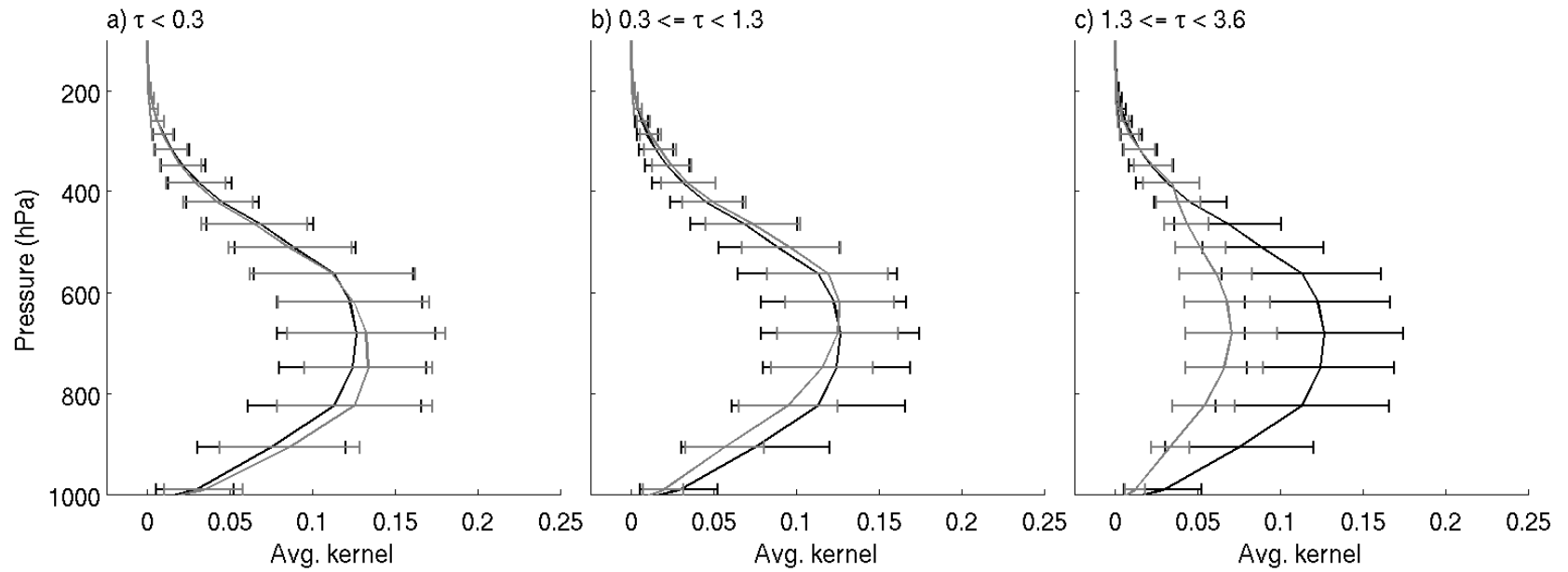
1



2

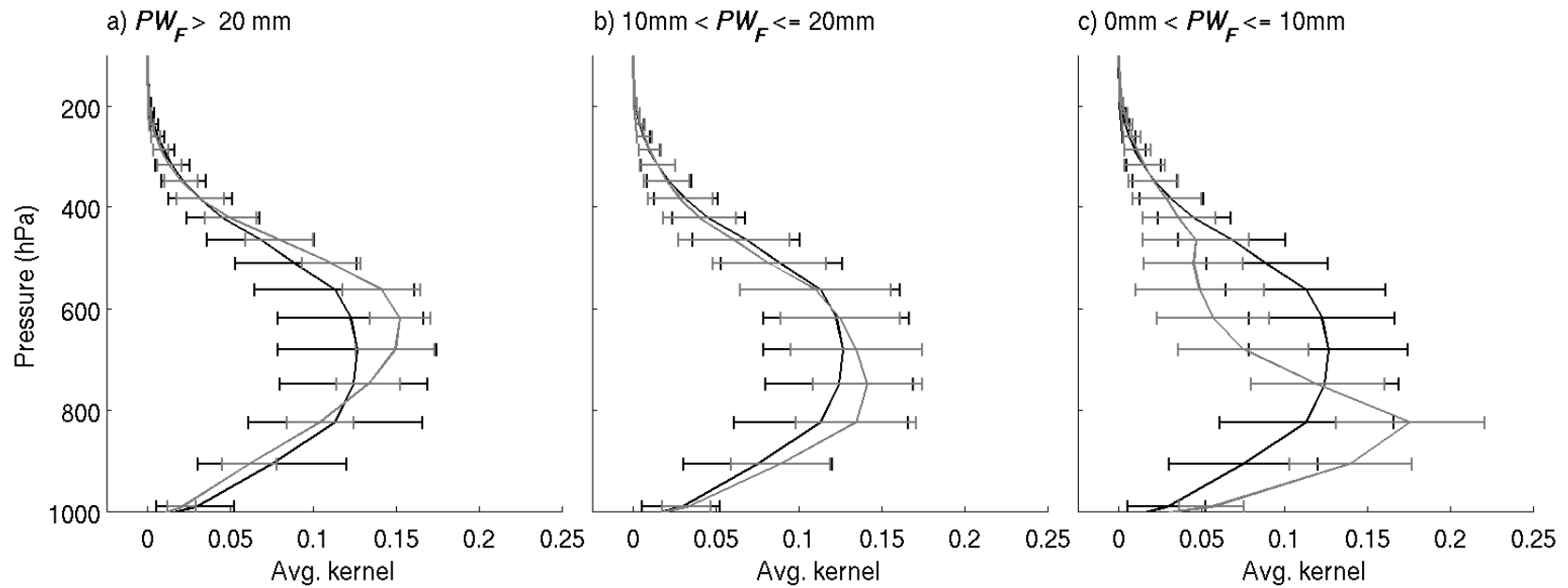
3 Fig. 5. Same as Fig. 4, but with control variables from TES replaced with those from ModelE. Black dashed lines show the
4 corresponding linear fits from TES observations in Fig. 4.

1



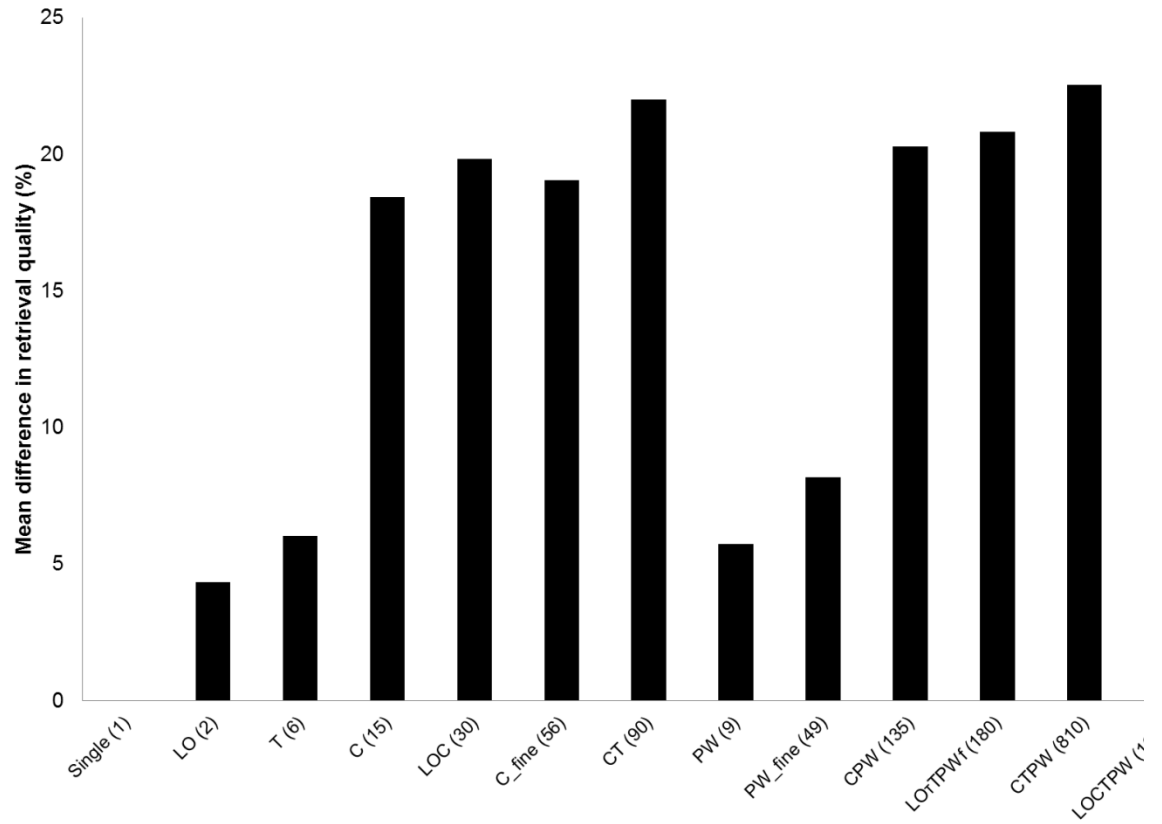
2

3 Fig. 6. HDO averaging kernel rows (grey) at 618 hPa for *CTP* less than 440 hPa and for τ a) less than 0.3 b) between 0.3 and 1.3 c) between 1.3 and 3.6. Black profiles
4 show the grand mean HDO averaging kernel row at 618 hPa across all high quality retrievals. Error bars show the standard deviation at each level. These averaging
5 kernels correspond to the first three entries in the top row of Table 4.



1

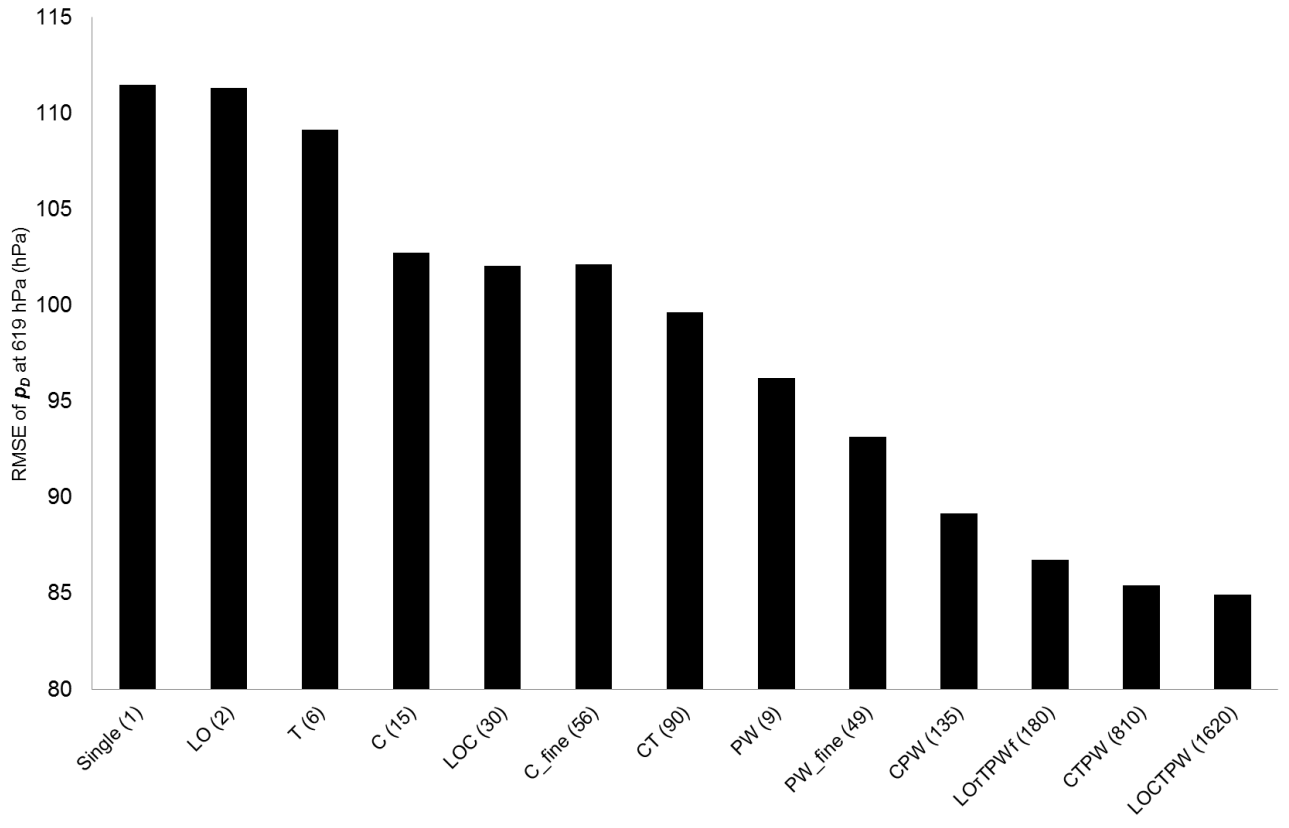
2 **Fig. 7. HDO averaging kernel rows (grey) at 618 hPa for CTP less than 440 hPa, τ less than 0.3, PW_B greater than 20mm, and PW_F : a) greater than 20mm (15%**
 3 **frequency, 81% quality) b) between 10mm and 20mm (14% frequency, 79% quality) c) less than 10mm (3% frequency, 82% quality). Black profiles show the grand**
 4 **mean HDO averaging kernel row at 618 hPa across all high quality retrievals. Error bars show the standard deviation at each level.**



1

2 Fig. 8. Mean difference between HDO retrieval quality within each category and the overall quality for the Single
 3 categorization (68%), for ~~eleven~~^{twelve} different categorizations. Differences are weighted by frequency of occur
 4 within each category. Numbers in parentheses indicate the total number of categories in each categorization.

5

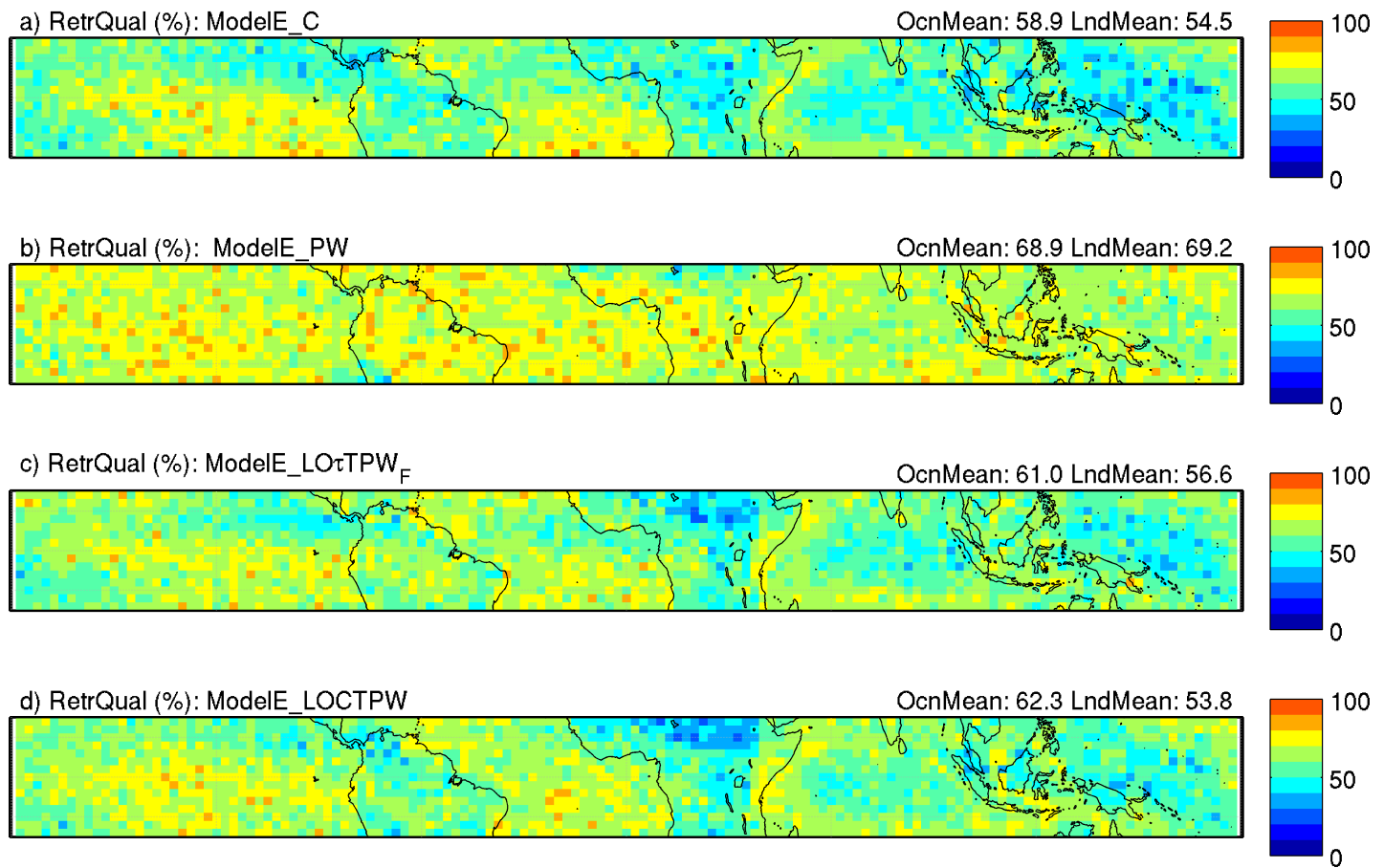


1

2 | Fig. 9. RMSE of p_D (height of peak HDO sensitivity) for the ~~eleven~~^{twelve} categorizations, and the 'Single' categorization.
 3 Numbers in parentheses indicate the total number of categories within each categorization.

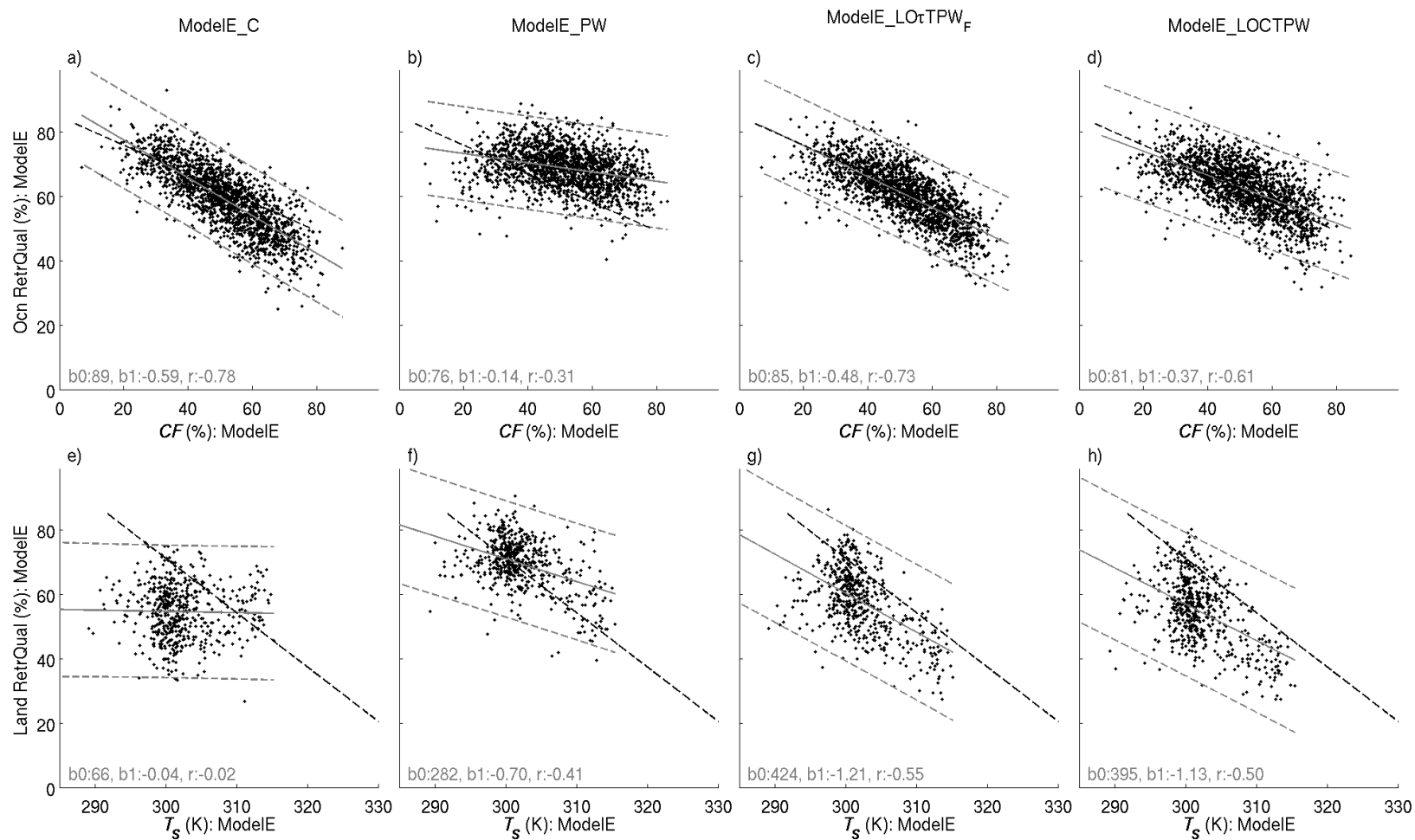
4

5



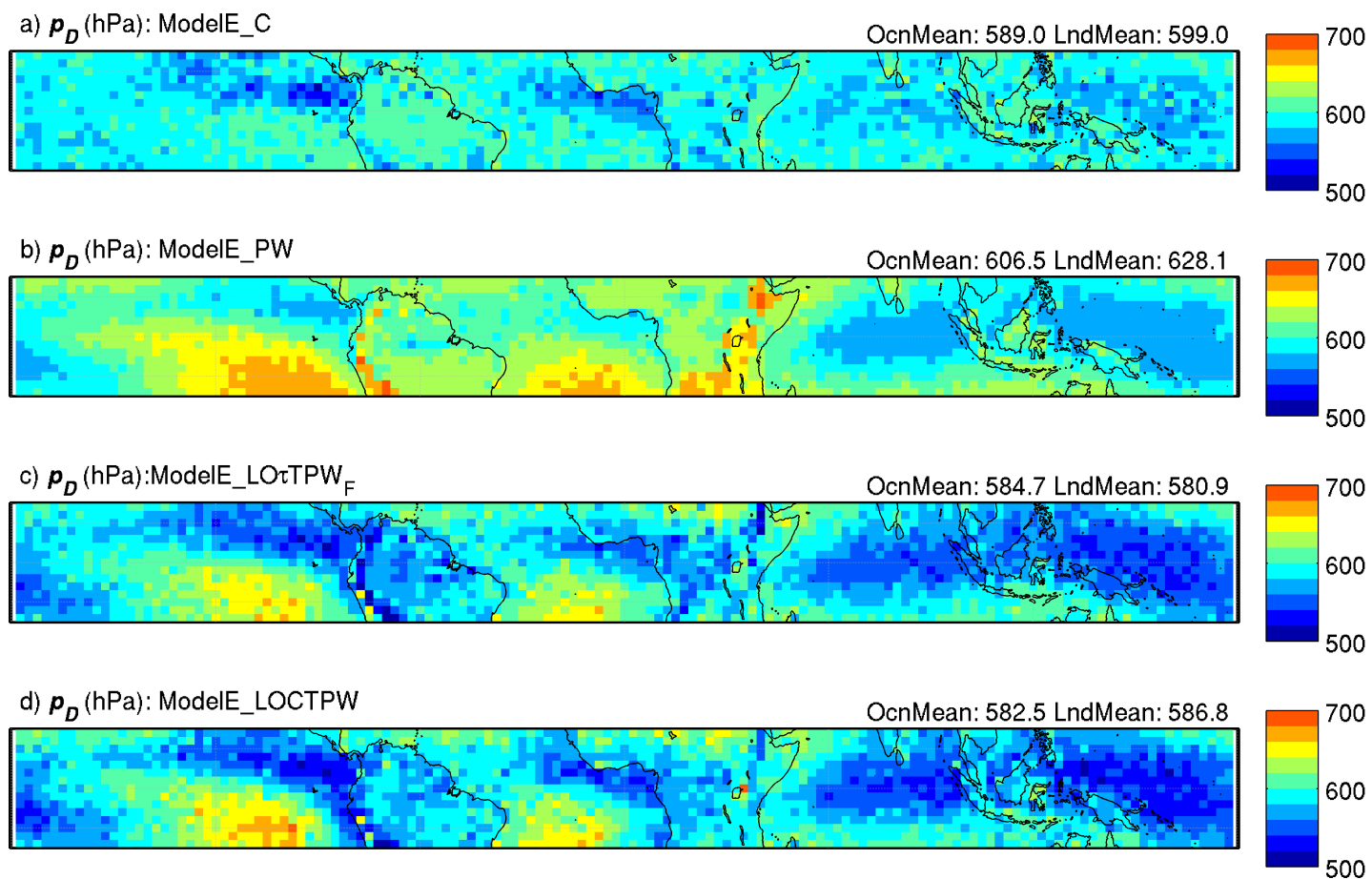
1

2 | Fig. 10. Approximated retrieval quality for ~~five~~four representative categorizations.



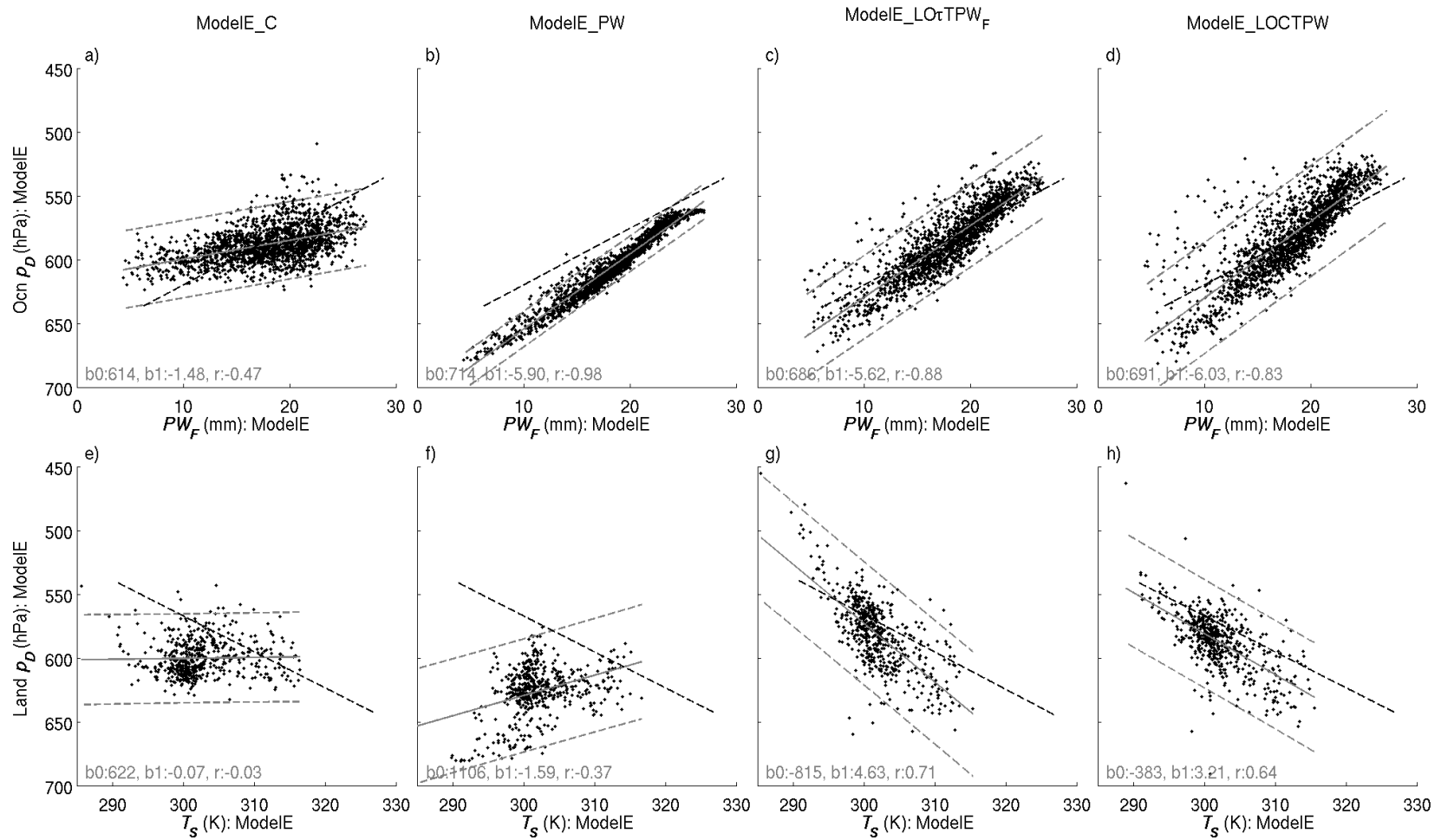
1

2 | Fig. 11. Approximated retrieval quality as function of CF over the ocean (top) and T_s over land (bottom) for ~~five~~ four representative categorizations. Grey dashed lines
 3 show the 95% prediction intervals. Black dashed lines show the corresponding linear fits from TES observations in Fig. 4a and Fig. 4c.



1

2 | Fig. 12. Approximated p_D (height of peak HDO sensitivity) for ~~five~~four representative categorizations.

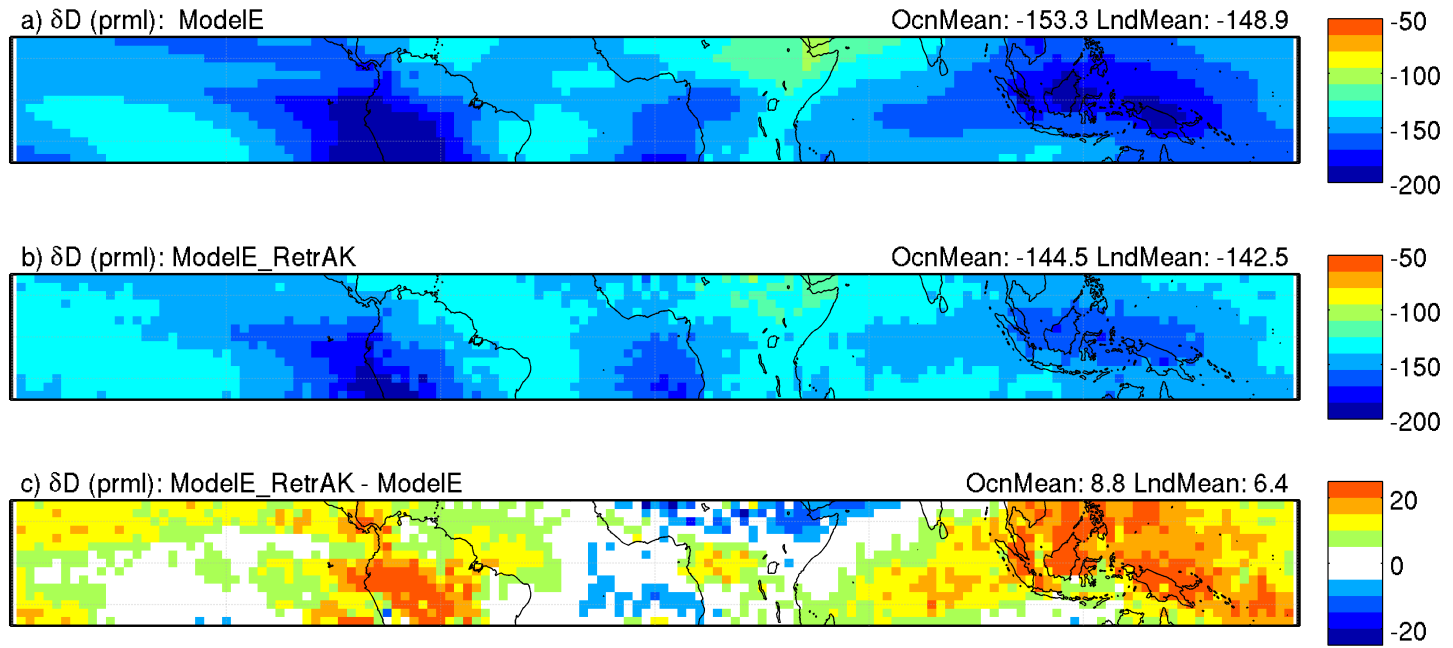


1

2 | Fig. 13. Approximated p_D (height of peak HDO sensitivity) as a function of PW_F over the ocean (top) and T_S over land (bottom) for **five-four** representative
3 categories. Grey dashed lines show the 95% prediction intervals. Black dashed lines show the corresponding linear fits from TES observations in Fig. 4b and Fig.
4 4d.

1

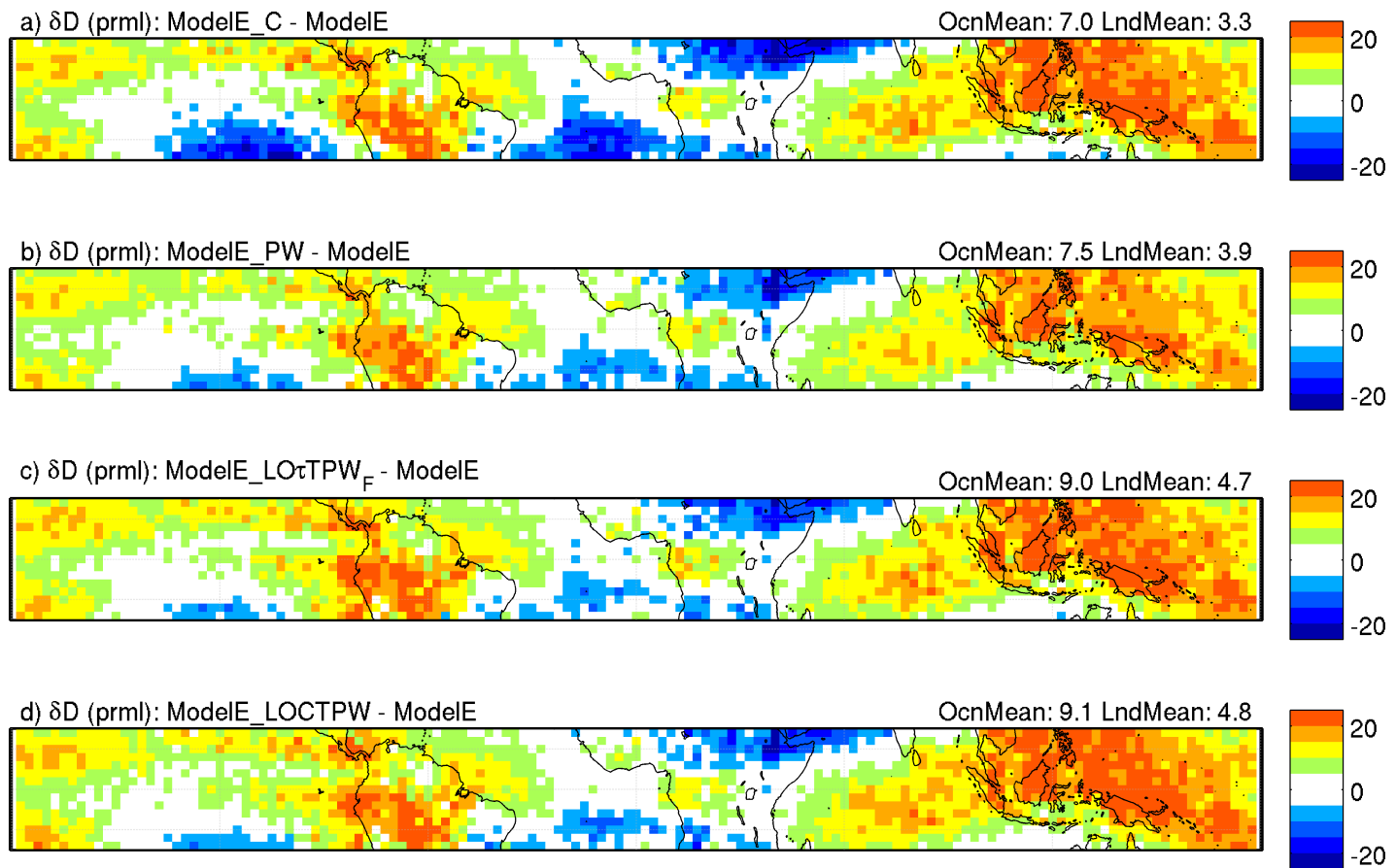
2



3

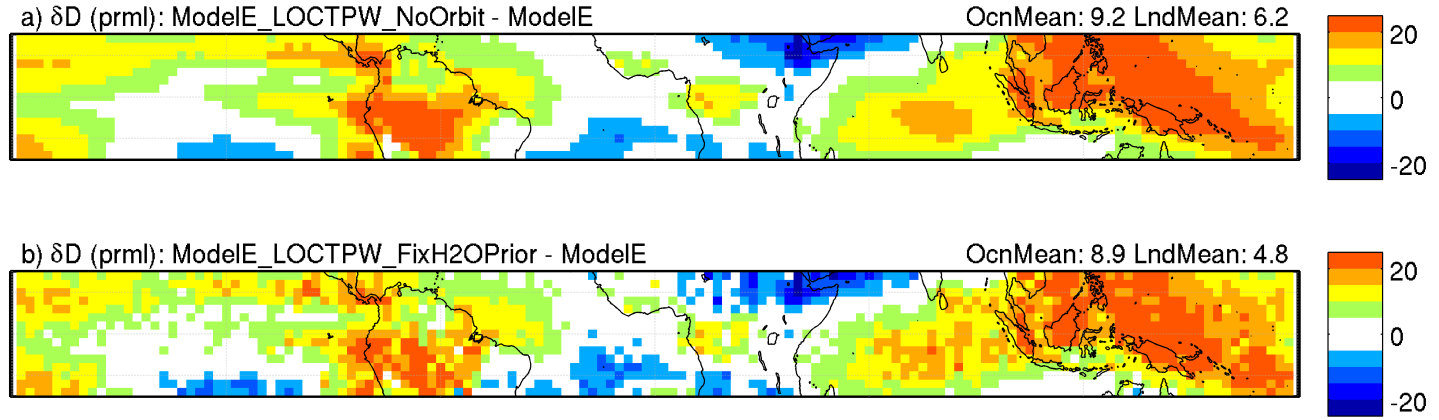
4

5 **Fig. 14. a) Raw ModelE vapor δD between 825 and 511 hPa during 2006 and 2009 for all months b) ModelE vapor δD after application of the retrieval based operator**
6 **c) difference between b) and a). The vertical mean of δD is weighted by specific humidity and pressure.**



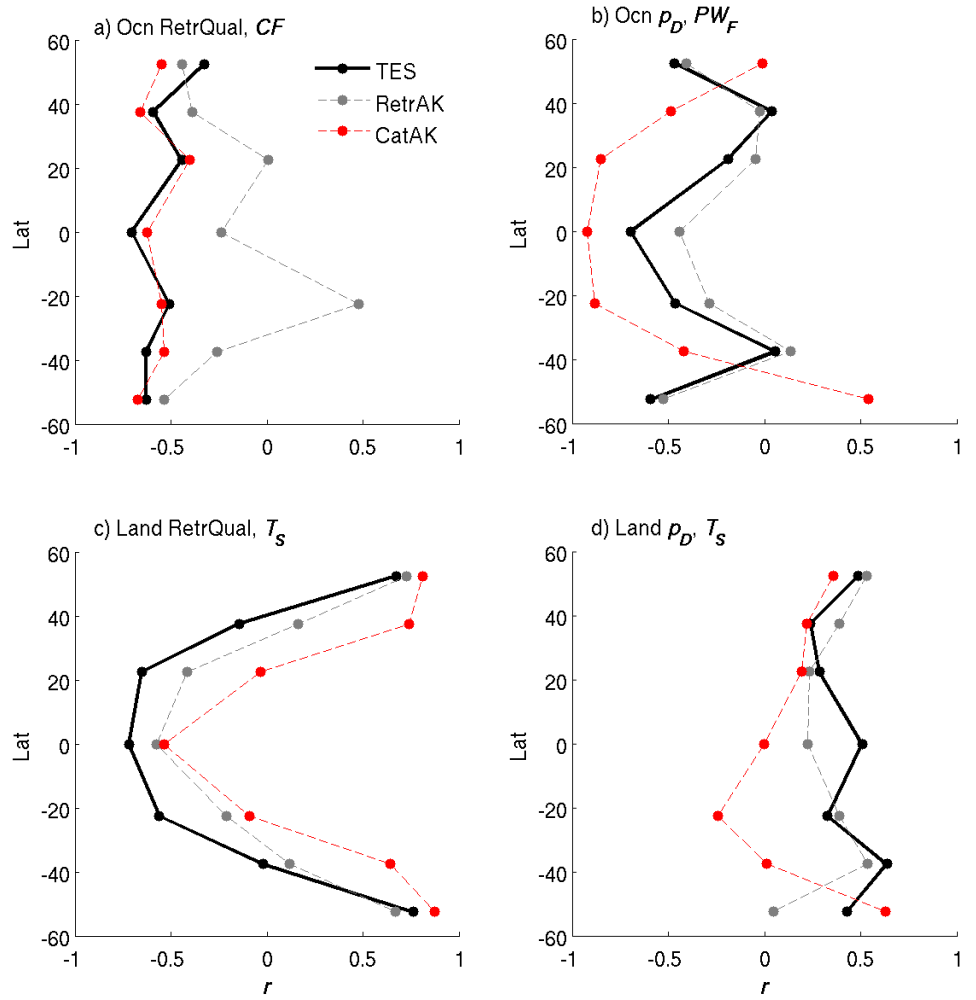
1

2 | Fig. 15. Same as Fig. 14 c), but for the categorical TES operator with the ~~five~~-four representative categorizations.



1

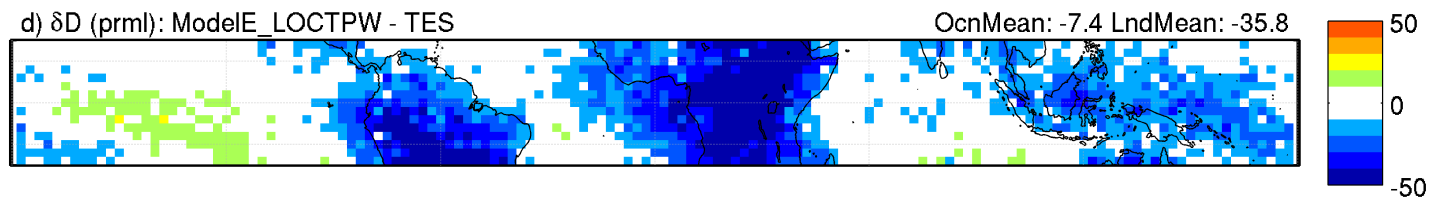
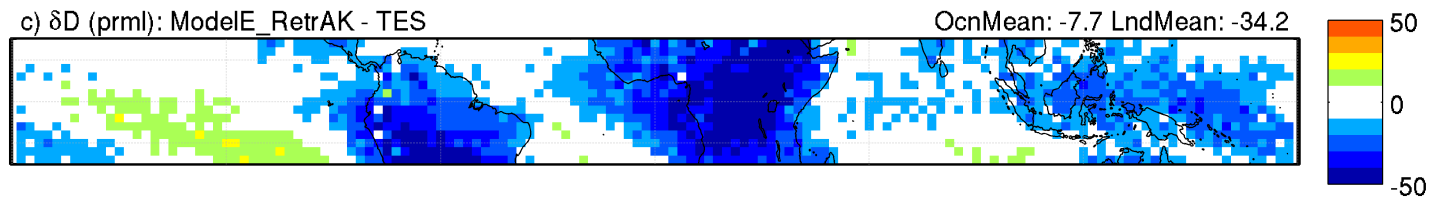
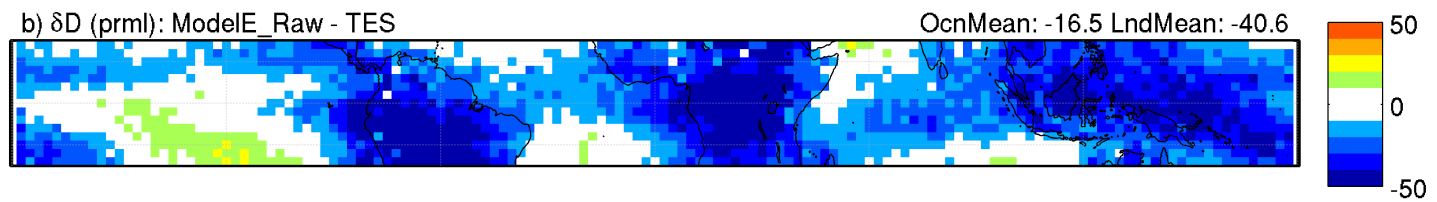
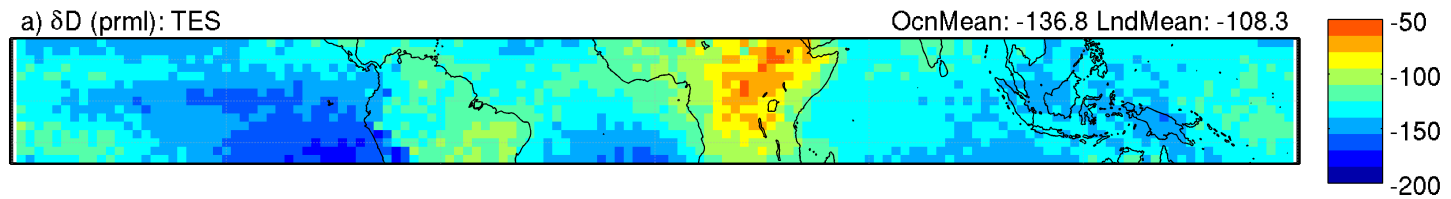
2 Fig. 16. Same as Fig. 15, but for two LOCTPW sensitivity tests: a) full daytime sampling and not just along the orbital path b) a fixed H₂O prior.



1

2 **Fig. 17. Correlation between retrieval quality and p_D (height of peak HDO sensitivity) with primary predictor vari**
 3 **over different latitudes.**

1



2

3 **Fig. 18. a) Retrieved TES δD (%).** Difference between ModelE and TES for: b) raw model δD c) model δD after applying the retrieval-based operator d) model δD after
4 applying the LOCTPW categorical operator.